AD-A155 083 MEASURING THERMAL PERFORMANCE OF BUILDING ENVELOPES: NINE CASE STUDIES(U) COLD REGIONS RESEARCH AND ENGINEERING LAB HANOVER NH S N FLANDERS MAR 85 1/1

UNCLASSIFIED CRREL-85-7 F/G 13/13 NL

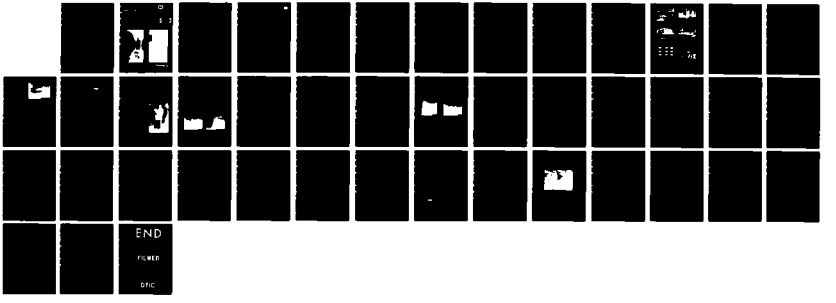

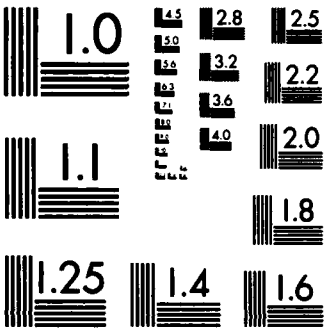

CRREL REPORT 85-7

US Army Corps of Engineers
Cold Regions Research & Engineering Laboratory

Measuring thermal performance of building envelopes

Nine case studies

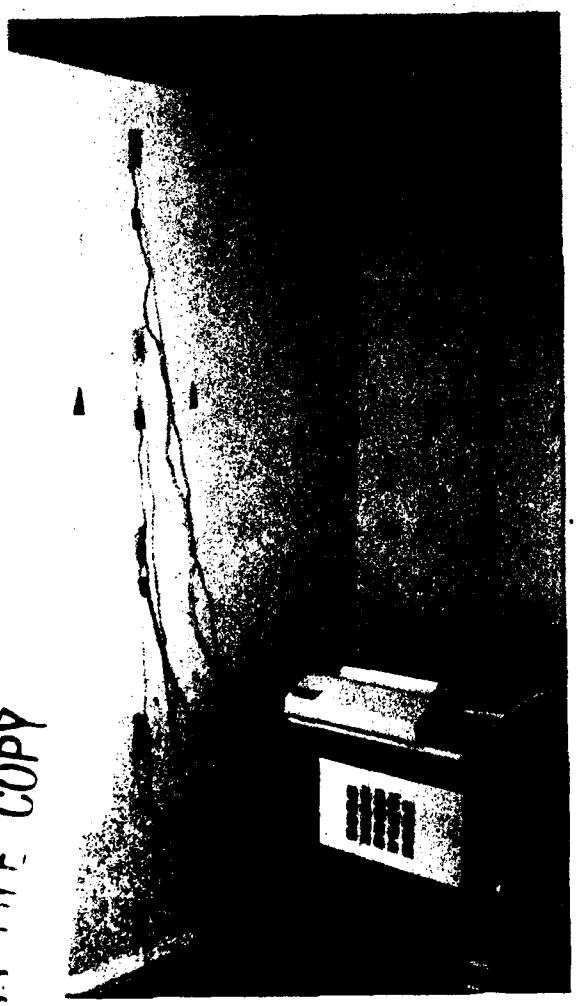

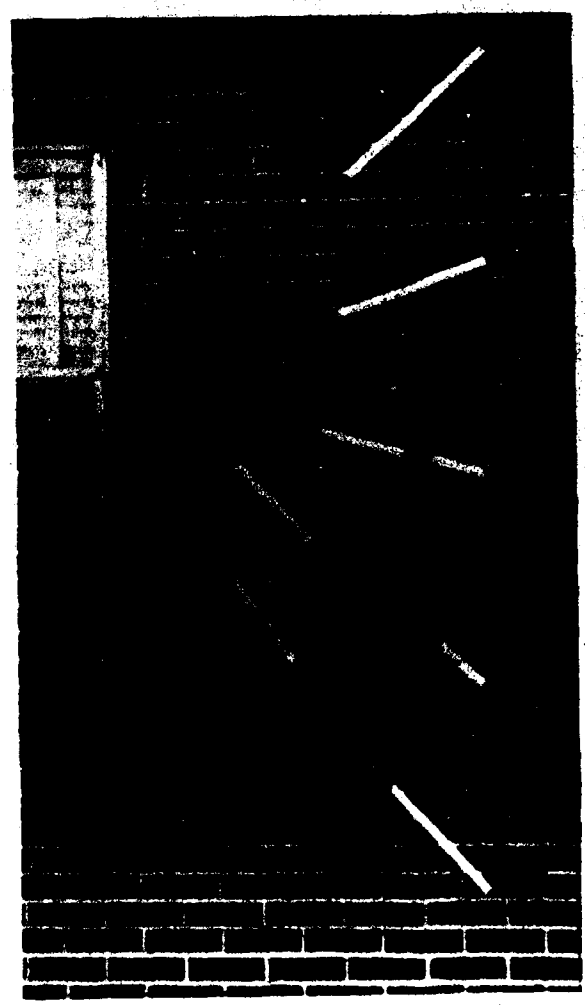

CONVERSION FACTORS: U.S. CUSTOMARY TO METRIC (SI) UNITS OF MEASUREMENT

These conversion factors include all the significant digits given in the conversion tables in the ASTM *Metric Practice Guide* (E 380), which has been approved for use by the Department of Defense. Converted values should be rounded to have the same precision as the original (see E 380).

Multiply	*By*	*To obtain*
British thermal unit	1055.056	joule
degrees Fahrenheit	$t_{°C} = (t_{°F}-32)/1.8$	degrees Celsius
foot	0.3048*	metre
gallon	0.003785412	cubic metre
inch	0.0254*	metre

* Exact.

Cover: Inside and outside surfaces of a wall during testing.

CRREL Report 85-7

March 1985

Measuring thermal performance of building envelopes

Nine case studies

Stephen N. Flanders

Prepared for
OFFICE OF THE CHIEF OF ENGINEERS
Approved for public release; distribution is unlimited.

Unclassified

SECURITY CLASSIFICATION OF THIS PAGE *(When Data Entered)*

REPORT DOCUMENTATION PAGE

READ INSTRUCTIONS BEFORE COMPLETING FORM

1. REPORT NUMBER: CRREL Report 85-7	2. GOVT ACCESSION NO.
3. RECIPIENT'S CATALOG NUMBER	
4. TITLE *(and Subtitle)*: MEASURING THERMAL PERFORMANCE OF BUILDING ENVELOPES Nine Case Studies	5. TYPE OF REPORT & PERIOD COVERED
	6. PERFORMING ORG. REPORT NUMBER
7. AUTHOR(s): Stephen N. Flanders	8. CONTRACT OR GRANT NUMBER(s)
9. PERFORMING ORGANIZATION NAME AND ADDRESS: U.S. Army Cold Regions Research and Engineering Laboratory, Hanover, New Hampshire 03755-1290	10. PROGRAM ELEMENT, PROJECT, TASK AREA & WORK UNIT NUMBERS: DA Project 4A762730AT42; Task C; Work Unit 010
11. CONTROLLING OFFICE NAME AND ADDRESS: Office of the Chief of Engineers, Washington, D.C. 20314	12. REPORT DATE: March 1985
	13. NUMBER OF PAGES: 42
14. MONITORING AGENCY NAME & ADDRESS *(if different from Controlling Office)*	15. SECURITY CLASS. *(of this report)*: Unclassified
	15a. DECLASSIFICATION/DOWNGRADING SCHEDULE

16. DISTRIBUTION STATEMENT *(of this Report)*

Approved for public release; distribution is unlimited.

17. DISTRIBUTION STATEMENT *(of the abstract entered in Block 20, if different from Report)*

18. SUPPLEMENTARY NOTES

19. KEY WORDS *(Continue on reverse side if necessary and identify by block number)*

Cost analysis; Thermal insulation; Economic analysis; Thermal measurement; Heat flow sensors; Energy Conservation; Insulation; Life cycle costs; END

20. ABSTRACT *(Continue on reverse side if necessary and identify by block number)*

Nine buildings at Ft. Devens were the object of a study employing heat flux sensors, thermocouples, a computer-controlled data acquisition system and infrared thermography. The purpose was to measure the R-values of those buildings to determine their economic potential for improved insulation. The sample included four frame buildings, two masonry buildings, and three frame buildings with brick facing. The technique for measuring R-values proved repeatable and accurate within 15%. Sampling a small representative sample sufficiently characterizes the entire stock of buildings. Measurement is more important for poorly insulated buildings, since the beginning R-value has a drastic impact on the budget for a cost-effective reinsulation project. At Ft. Devens, installing an external Styrofoam insulation system on concrete block barracks has a savings-to-investment ratio of about 1.4. Additional keywords:

DD FORM 1 JAN 73 1473 EDITION OF 1 NOV 65 IS OBSOLETE

Unclassified

SECURITY CLASSIFICATION OF THIS PAGE *(When Data Entered)*

PREFACE

This report was prepared by Stephen N. Flanders, Research Civil Engineer, Civil Engineering Research Branch, Experimental Engineering Division, U.S. Army Cold Regions Research and Engineering Laboratory. This study was conducted as a part of DA Project 4A762730AT42, *Design Construction and Operations Technology for Cold Regions.*

The author acknowledges the dedicated assistance of his colleagues. Brian Harrington helped develop the field procedure for installing the monitoring equipment. Todd Carpenter developed the data acquisition program that made the data collection possible. Ronald Domingue helped in a variety of ways, including performing studies on different aspects of the collected data. Doris Van Pelt helped calibrate the sensors used in the study.

The author is also grateful for the cooperation of the Facilities Engineering and Housing staff of Ft. Devens for making the study possible. They include John Grafton, Carl Seely, Joseph Tammaro and Karl Uebersohn.

The author thanks Barry Coutermarsh and Charles Korhonen, both of CRREL, and Brian Rennex of the National Bureau of Standards who reviewed this report for technical content.

CONTENTS

ILLUSTRATIONS

Figure

TABLES

MEASURING THERMAL PERFORMANCE OF BUILDING ENVELOPES
Nine Case Studies

Stephen N. Flanders

INTRODUCTION

Building owners and operators have been investing in energy conservation improvements for more than a decade now. Some are easy to justify with confidence. Building insulation is the ultimate defense against losing energy to the outside in winter or gaining unwanted energy in summer through walls, roofs and floors. However, there is no broad body of experience that shows whether building envelopes generally perform according to expectations. If the actual performance is different than expected, then organized measurements of suspect buildings could determine their economic potential for thermal improvement. To achieve the broad experience, a reliable measurement process is the first step.

This is a progress report on the effort at CRREL to:

1) Develop a reliable technique for measuring the thermal performance of building envelopes, primarily using laboratory experiments.

2) Build experience in the differences between actual thermal performance and those expected from handbook values, resulting from a field study of nine buildings at Ft. Devens, Massachusetts, during February and March 1982.

3) Characterize the economic potential for investments in building envelope thermal improvements, drawing on the results of the field study and the economic constraints on investment in Ft. Devens' physical plant.

Sensing heat flow and surface temperature is the foundation of the measurement process. The tools include contact sensors (thermocouples and thermopiles) and infrared thermal imaging equipment. This equipment requires calibration appropriate for the desired measurement. This report includes studies to characterize the sensitivity of thermal sensors to their environments: How constant is their calibration?

Knowledge of where to measure, how long to measure, how to generalize a local result, and how to interpret the data is essential for a meaningful investigation. The technique employs infrared thermography for locating either typical or anomalous points for placing sensors.

Temperature sensors on inside and outside surfaces measure the potential for heat flow through the thickness of the structure. Heat flow sensors on the inside surfaces also indicate whether a change in temperature potential across the structure translates rapidly or sluggishly into a change in heat flow, depending on the thermal resistance and the storage properties of the materials. The sensors respond to their immediate surroundings. However, they may be placed where heat doesn't flow directly through the thickness of the structure

but can flow laterally due to a less resistive path or due to convection. Thermography may detect the potential for this problem.

An accurate measurement of thermal resistance (R-value) when temperatures are changing depends on the thermal properties of the building section and the thermal conditions during the measurement. This is a function of the thermal storage properties of the building section delaying the heat flow that results from a change in temperature potential across the section. The most reliable means to assure a sufficient accumulation of data is to employ a computer that tests data frequently to determine convergence of the R-value calculations on a constant value.

In some cases it may be appropriate to use thermography to map the variation in thermal properties over a broader area than the vicinity of the sensor. With sensors placed at thermal extremes within a region, thermography permits interpolation of intermediate thermal values at other locations.

Interpretation of the data depends on the objective for obtaining it. In cold regions the dominant thermal performance quality of interest is R-value. When the outside temperature fluctuates around the balance point (the temperature at which there is no heat gain or loss through the envelope), the thermal time constant of the construction is of interest. If the field data are being obtained to validate a response factor computer model, then certain key frequency domains of the data are of interest.

The Army has been actively pursuing energy conservation investments in order of attractiveness. Reinsulation projects don't often receive top priority, even in cold climates, because the cause of energy loss is spread out over a large area and the investment per unit can be high compared to other energy-saving measures. Any consideration of existing insulating qualities and possible improvements currently relies on handbook and manufacturers' data. The thermal survey of nine buildings at Ft. Devens consisted of comparing the results of R-value measurements with the theoretical R-values obtained from ASHRAE *Handbook of Fundamentals* calculations.

The investor in energy conservation should try to save the most energy cost for the least construction cost. If the actual performance of either the original construction or the proposed improvement is significantly different from what handbook or manufacturers' data suggest, the return on investment will be different also. This study looks at the potential for adding insulation to nine buildings, according to life-cycle cost (LCC) analysis and the Energy Conservation Investment Program (ECIP), which funds much of the Army's improvements. LCC analysis can determine whether the cost of reinsulation justifies the savings in energy operating costs.

FIELD INVESTIGATION

The thermal performance of building envelopes at Ft. Devens was investigated during the first few months of 1982. The effort concentrated on family housing units, bachelor officers' quarters and visiting officers' quarters. Because of the scheduled refurbishment between occupancies, unoccupied quarters were available for the research.

There were several phases of work. In January a thermographic survey gave an overview of the thermal performance of different types of construction on the base. During February and March a case-by-case survey of nine quarters involved both thermography and thermal measurements with heat flow and temperature sensors. Laboratory calibrations of sensors and analysis of the field data completed the investigation.

Overview study

The overview thermographic study took place on 5 and 6 January 1983, when outdoor temperatures were around freezing and above. The study included both frame and masonry buildings. Unlike Korhonen and Tobiasson's (1978) experience with low-slope roofing systems, infrared inspection of building walls revealed very few anomalies. One of the few apparent anomalies was actually a variation in surface emissivity. Details from this overview study were used in the nine case studies.

The most important result was the apparent consistency of performance among buildings of similar construction. A small sample of similar buildings on a military installation will apparently represent the entire population of like buildings adequately. Subsequent measurements supported this hypothesis.

Case study building types

The case study encompassed five building types: two frame constructions, two masonry constructions and one combination of masonry and frame. While the buildings studied were primarily residential, the wall constructions are similar to much of the Army's building stock.

Figure 1 shows typical examples of each building type. For convenience some types are referred

a. Capehart family housing.

b. Wherry family housing.

c. MCA bachelor officers' quarters.

d. MCA family housing unit.

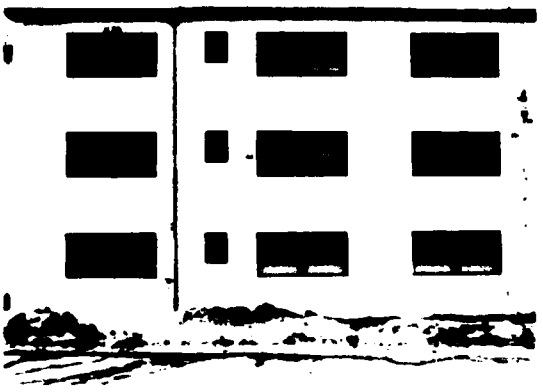

e. Masonry block visiting officers' quarters.

f. Brick colonial officers' dwelling.

Figure 1. Examples of the building types studied at Ft. Devens.

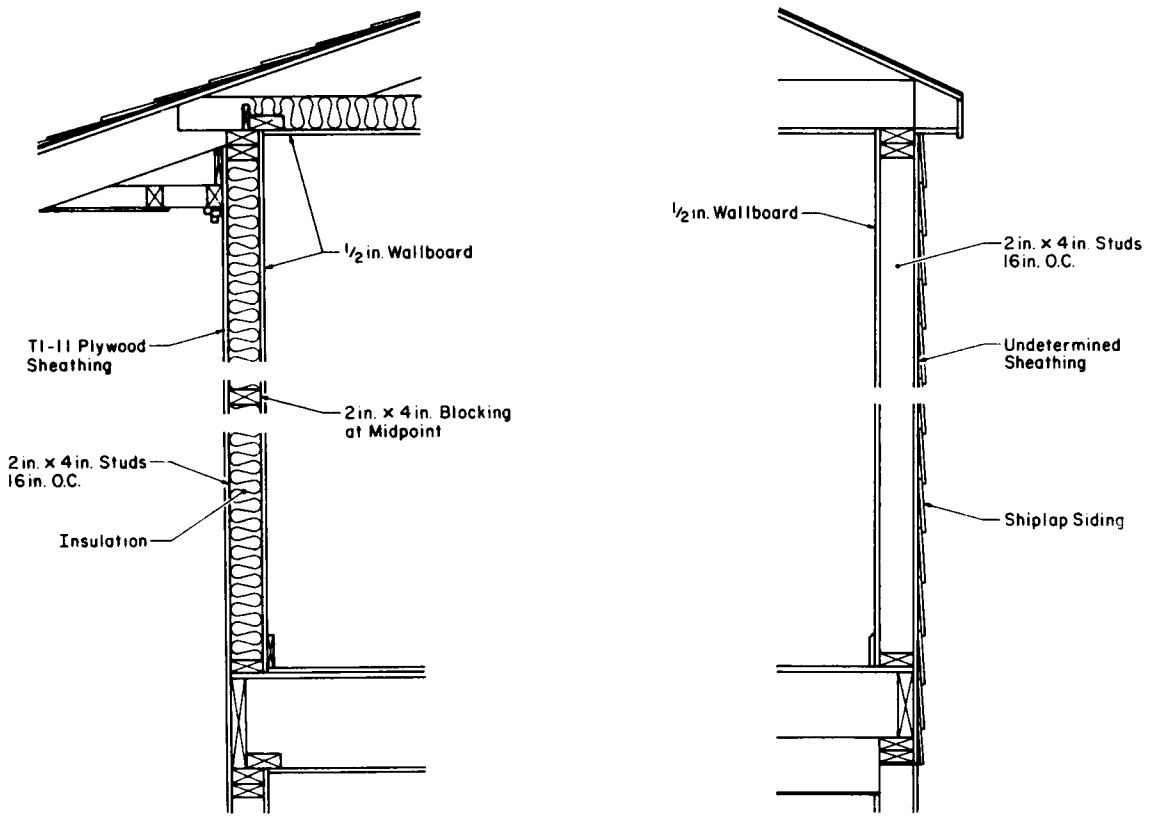

a. Capehart building. *b. Wherry building.*

Figure 2. Typical cross sections of frame buildings at Ft. Devens, according to as-built drawings and external inspection.

to by the names of the funding program under which they were built: Capehart, Wherry and MCA. "Colonial" refers to the style of masonry building studied. The only other type was concrete block.

Table 1 summarizes the building types. As-built drawings and observation of exterior surfaces were the primary sources of information about the construction. The finished surfaces were not penetrated to confirm interior layers of materials. Subsequently, verification holes of similar buildings established what the construction was in most cases.

The Capehart buildings were typically eight-unit townhouses. Figure 2 represents the as-built cross section. The measurements of the two examples of this type were in equivalent locations in the buildings. Note the 2 in. of fiberglass batt insulation in the wall mid-depth in the stud space. Subsequent borings revealed 3.5 in. of fiberglass batt insulation.

Table 1. Summary of case study construction types. R-values are calculated handbook values, from interior to exterior surface. For some roofs an R-value was neither calculated nor studied.

Construction	*Name*	*R-values**		*No. of surveys*
		Wall	*Roof*	
Frame	Capehart	9.8	13,19	2
	Wherry	2.9	21	2
Frame/masonry	MCA1	9.9	-	1
	MCA2	14	15	2
Masonry	Conc. Block	3.2	-	1
	Colonial	3.2	-	1

* (°F hr ft²/Btu).

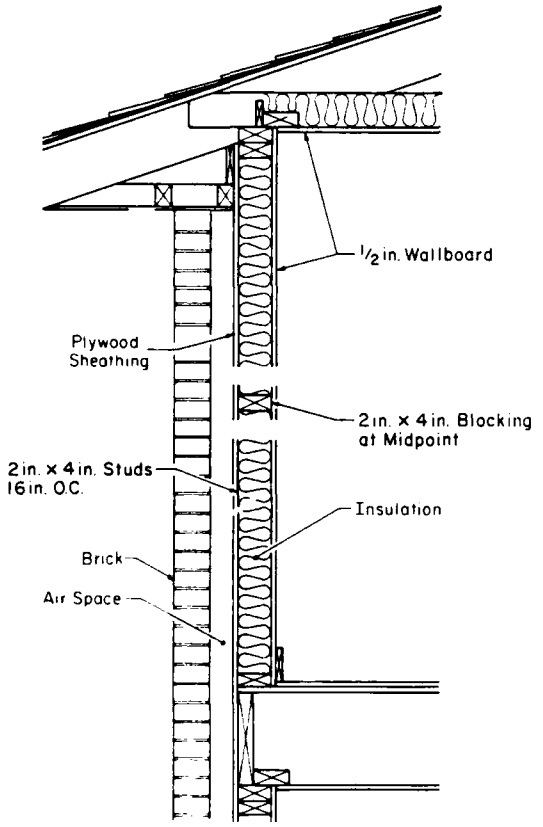

Figure 3. Typical cross section of MCA buildings at Ft. Devens, according to as-built drawings.

The Wherry houses were also townhouses, with a brick veneer on the first floor. The thermal measurements were on the second floor only, where the exterior cladding was shiplap. The as-built drawing (Fig. 2) shows no insulation within the stud space in the wall. Both frame construction types had attics with insulation between the ceiling joists.

A denotes the brick veneer frame construction shown in Figure 3. According to the as-built drawing, the insulated cavity had 2 in. of fiberglass insulation applied to the warm side of the 3.5-in. stud cavity. Borings revealed insulation for the full 3.5 in. The roof construction sometimes included attics, which were inaccessible in the locations visited, and sometimes cathedral ceilings.

The concrete block building has two layers of 4-in. concrete masonry with a 2-in. air space between, as shown in Figure 4. No roof measurements were made of this structure.

The colonial house was of brick and terra cotta masonry, shown in conjectural cross section in Figure 4 because no detailed, as-built drawings exist. No roof measurements were made of this structure.

These categories represent an upper and a lower level of insulation for the frame and brick veneer construction types and represent a range of construction types from thermally light to thermally massive. In most cases there were at least two examples of the same construction type to test whether the measurement technique is reproducible.

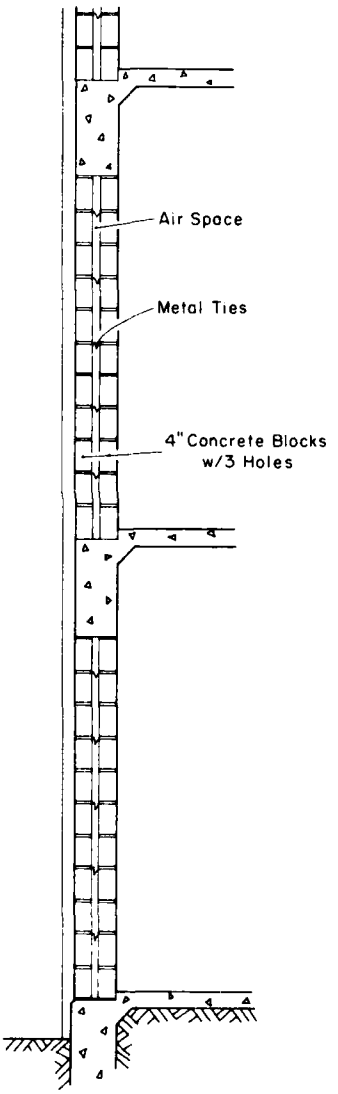

a. Concrete block building.

Figure 4. Typical cross sections of masonry buildings at Ft. Devens, according to as-built drawings.

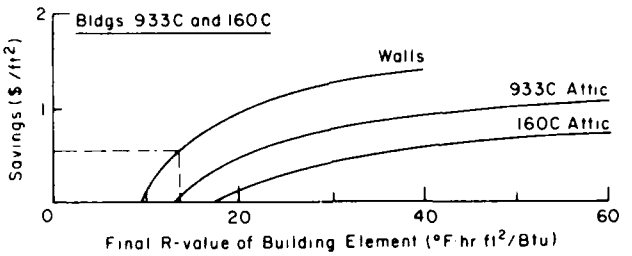

Figure 13. Fifteen-year present worth energy savings potential for adding insulation to two Capehart buildings as a function of the final R-value.

obtained as an average figure from the office that purchases fuel.* The calculations further assume

Flanders (1982) developed a concept called a climate-heating cost parameter (CHC). This value (eq 3) reflects fuel cost, heating plant efficiency, heating degree-days, and the present worth factor for the fuel costs over the time period of interest. In $ hr °F/Btu for Ft. Devens

$$CHC = 24 \times (HDD)(P/B)(F) = 17.48 \quad (3)$$

where 24 = factor converting days to hours
HDD = 6475 heating degree-days (based on 65 °F)
P/B = 11.36, present worth factor for an escalating series for a 15-year period (Table 1 in ECIP 1982)
F = $9.90/10⁶ Btu, cost of fuel, adjusted for plant efficiency.

Equation 3 neglects the internal gains from the building and the cost of heat plant capitalization and maintenance.

CHC, when multiplied by the Btu/°F hr performance improvement anticipated, yields dollar values of the energy cost savings in terms of present worth. In the case of improving insulation performance, the savings are

$$S = (\Delta U)(CHC) \quad (4)$$

where $\Delta U = U_{in} - U_{af}$
U_{in} = initial conductance (Btu/°F ft² hr or Btu/°F hr)
U_{af} = conductance after insulation is added.

*Personal communication with E. Poulin, Ft. Devens, 1983.

S is the break-even value for investing in upgraded insulation acceptable under ECIP. This yields a Savings-to-Investment Ratio (SIR) of 1.0. To obtain an SIR of 2.0, one would have to spend half of *S* on the insulation improvement project.

Savings potential in Capehart buildings

The Capehart wood frame buildings showed the least potential for improvement, as Figure 13 demonstrates. The walls are nearly, if not totally, full of insulation, so any additional potential improvement would probably accompany a cladding project. Such a project would have a budget of approximately $0.50/ft² to add R-3.6 (about an inch of expanded polystyrene insulation) to the building exterior and achieve an SIR of 1.0 with an economic lifetime of 15 years. A period of 25 years would allow a $0.75/ft² investment. Reynolds et al. (1981) suggested in their analysis of insulation projects for Ft. Devens that such insulation would not qualify economically. Their figures suggest that an additional R-13 or 4 in. of blown-in insulation might be economical in the attic, but with a low SIR.

Savings potential in Wherry buildings

The Wherry buildings have a significant economic potential for thermal improvement in the walls but not in the attics. Filling the walls with insulation would have a break-even budget of about $4.10/ft² for 15 years (Fig. 14) yet might only cost about $1.25/ft² (this is Reynold's estimate of $0.92/ft² in 1980 escalated to 1983). That would represent an SIR of 3.3. These buildings have a brick veneer on the lower story that may make blown-in insulation more difficult to install and exterior insulation and cladding more difficult either to match with the brick or to justify for the entire wall area.

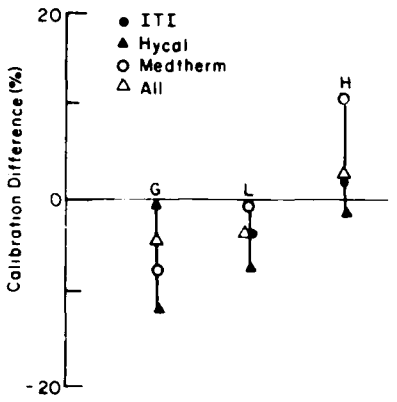

Figure 12. Average difference in calibration between a reference set of calibration runs and the test condition for all treatments of each sensor type. G = *gypsum wallboard;* L = *polystyrene foam with a low R-value;* H = *polystyrene foam with a high R-value.*

constants that were between four and eight times greater than the manufacturer's numbers. There were no special calibration figures for concrete or plaster, which were encountered in two of the nine buildings measured at Ft. Devens.

Heat flow sensor sensitivity

After the sensors were calibrated, their sensitivity to the thermal conductivity of the surface they were placed on was tested. In this case the test surface consisted of the 2-in. thickness of extruded polystyrene foam without the gypsum wallboard. Since Schwerdtfeger (1970) demonstrated that the ratio of thermal conductivities between an HFS and its surroundings affects how much heat flow the sensor reads, the fact that gypsum wallboard is nearly six times more conductive than the polystyrene may affect measurement accuracy. Using an adaptation of Schwerdtfeger's analysis (Appendix C), we might expect a 20–30% increase in heat flow measurements on a polystyrene surface over the gypsum wallboard, given equal overall conductances of the wall. This would result in a lower calculated R-value. The results showed no such significant effect. The calibration constants were obtained according to eq 2. The calibration constants for the foam alone were only 2.7% higher than for sensors placed on wallboard, but this difference is much less than the standard deviation of these tests.

A second series of three tests employed five sensors covered with tape as in the field, and three with a 12-in.-square cover of 0.5-in. gypsum wallboard or 0.375-in. plywood with an inset for the sensor and its leads. In addition, I employed another sensor type with an aluminum facing, similar in size to the first type with the same treatments. Lastly, I tested a larger sensor with only tape over it. Each test represented three conditions: a 2-in. thickness of extruded polystyrene foam with a 0.5-in. layer of gypsum wallboard pressed onto it with springboards, the same without the wallboard, and the original 2 in. of polystyrene with an additional 1 in. pressed onto it.

Figure 12 demonstrates that for all sensors and all treatments there was little difference between the calibration of sensors on sheetrock and on foam. There was a greater effect from having the second layer of foam. This result is suspect, however, because this condition was not part of the procedure that randomized the tearing down and setting up of experimental variables. Appendix D describes this study in greater detail.

We can conclude that heat flow sensors may be much less sensitive to surrounding thermal properties than Schwerdtfeger's analysis would suggest. From an adaptation of his analysis (Appendix C), there would have been almost a 30% difference in calibration constant between a polystyrene surface and gypsum wallboard. I observed an insignificant difference of about 3%. Likewise, a 30% difference in calibration between wallboard and concrete or plaster might be expected. I did not test this potential difference, but the difference may be as insignificant as between polystyrene and wallboard.

ENERGY CONSERVATION INVESTMENT POTENTIAL

The ultimate purpose of this measurement process is to determine the investment potential for improving building insulation. The potential differs according to the performance of the existing insulation and the cost of the heat energy it allows to escape. This report assumes that each building studied has its own heating plant, using distillate fuel oil with a heat content of 138.7×10^3 Btu/gal. This figure is mandated in Energy Conservation Investment Program (ECIP) Guidance dated 13 October 1982 and represents the midrange of values for no. 2 fuel oil found in ASHRAE (1977). The economic calculations assume a fuel cost of $1.03 per gal.

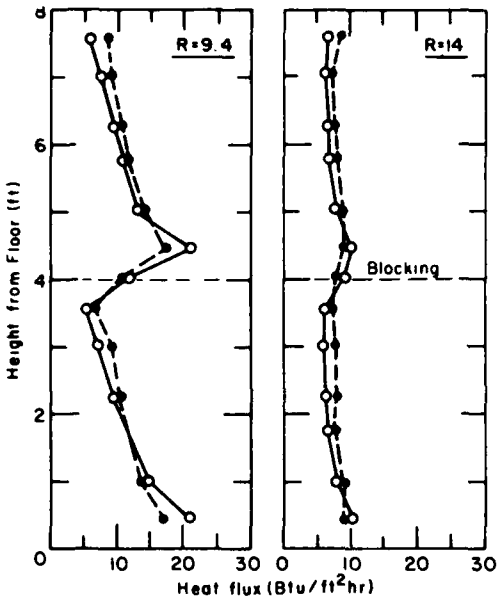

Figure 11. Heat flux through laboratory test wall sections. In the case on the left a single, vertical foil curtain creates two air spaces within the stud cavity. In the case on the right the wall contains a 2-in. mineral wool batt with an air space on the cold side. The open circles represent heat flux through the stud spaces, and the closed circles represent flux through the studs. Reproduced by permission of National Research Council of Canada.

has a primarily convective heat transfer mechanism, the resulting curve (Fig. 11a) would have the characteristics of Figures 10a and b. Where insulation is a dominant factor, curves correspond to Figure 11b.

SENSOR CALIBRATION

Two types of sensors were employed: thermocouple temperature sensors and thermopile heat flow sensors. The temperature sensors were checked for proper output by placing them in an ice bath and in boiling water to test for 32° and 212°F, respectively. The heat flow sensor calibration method was not so trivial, since it must reflect the conditions of use.

Heat flow sensor calibration

To simulate the conditions of measurement in the field, the calibration apparatus was a calibrated hot box. The box accommodates wall test sections up to 8 by 12 ft. The wall section employed for the calibration of the sensors was made of 2-in. tongue-and-groove extruded polystyrene taped at the joints with a layer of 0.5-in. gypsum wallboard held against the insulation with springboards.

Extruded polystyrene has well-documented thermal conductivity properties as a function of mean temperature. Gypsum wallboard represented about 2% of the overall thermal resistance, so any uncertainty about its thermal properties would have minimal impact on the assumed properties of the overall wall section used in the calibration. Gypsum wallboard was the material behind the HFS in all but two of the nine buildings measured.

A plan for randomized location of sensors on the calibration wall minimized the potential for bias due to anomalous properties of the wall or uneven distribution of temperature within the test chamber. The sensors were attached at new locations each day without stopping or resetting the refrigeration on one side of the chamber or the heating on the other.

A calibration constant was calculated from

$$Cal = (\Delta T_{ave}/SO_{ave})/R_{wall} \qquad (2)$$

where Cal = Calibration constant
ΔT_{ave} = Average difference in temperature across the test wall
SO_{ave} = Average HFS output
R_{wall} = Thermal resistance of the test wall.

The standard deviation resulting from moving the sensors from one location to another was only 2.4–2.7% of the average for any given sensor. Compared with the field results (Table 7), with standard deviations of between 10 and 87% of the means of the R-values for each group of sensors, this indicates that the variability of the field results reflected actual conditions and not merely inadequate control of measurement consistency.

Calibration of the HFSs according to the manner in which they were used resulted in conversion

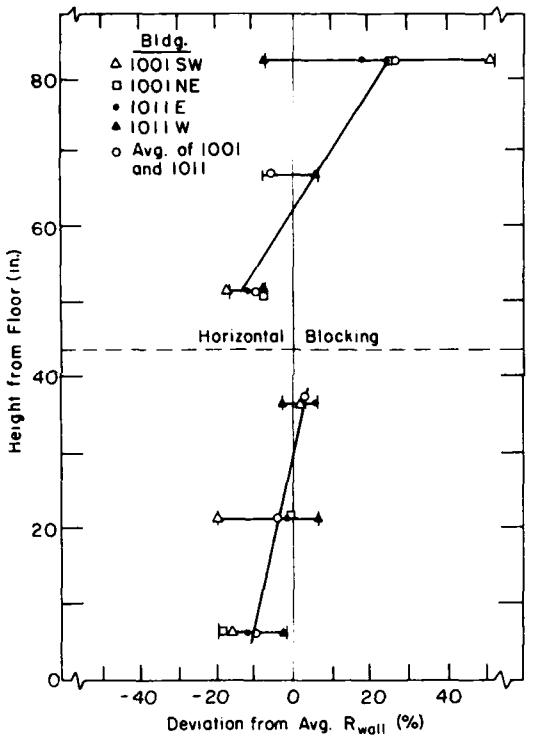

a. Wherry housing (buildings 1001 and 1011).

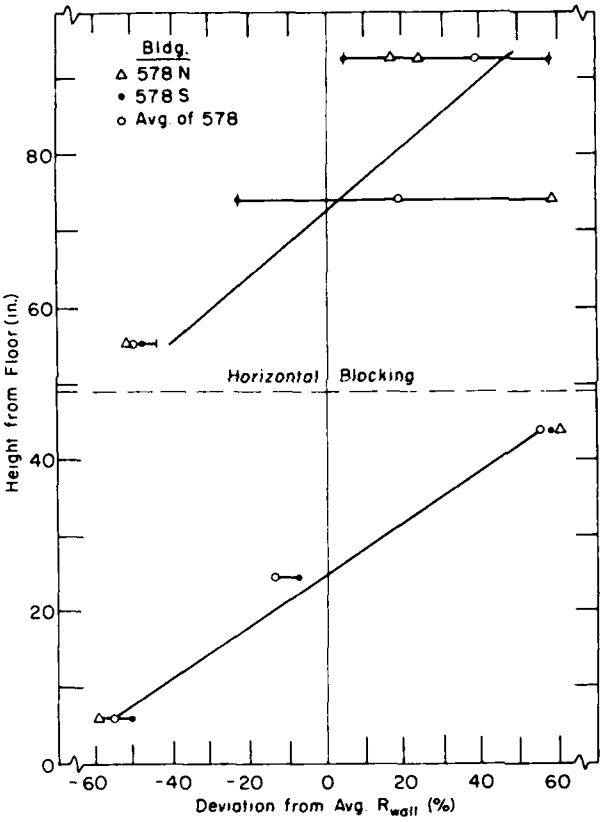

b. MCA housing (building 578).

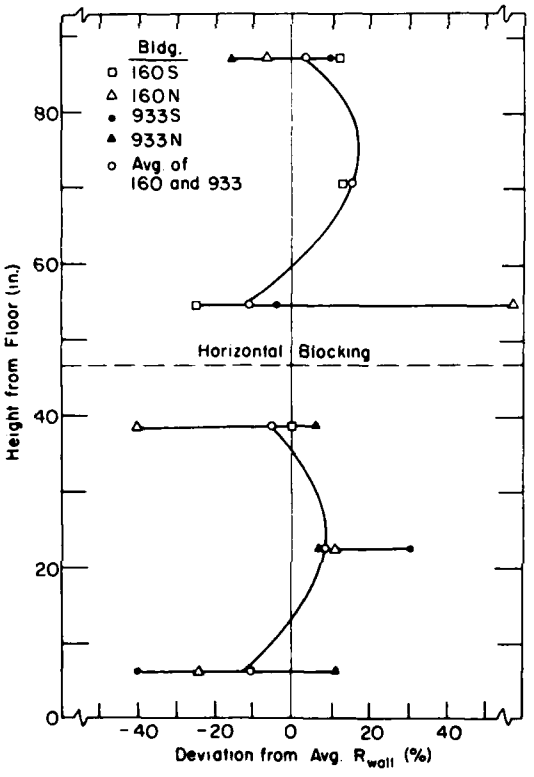

c. Capehart construction (buildings 160 and 933).

Figure 10. Percentage deviation of each R-value (R_{wall}) from the average R_{wall} for each wall, plotted against height on the wall.

Table 8. Standard deviation as a percentage of the means of the R-values obtained for each group of sensors shown. The number of values used in calculating the %S.D. is *n* for each orientation.

	Walls								*Roof*	
	North		*East*		*South*		*West*			
Building	*%SD*	*n*	*%SD*	*n*	*%SD*	*n*	*%SD*	*n*	*%SD*	*n*
Capehart:										
933	12	5	-	-	26	5	-	-	10	5
160	38	5	-	-	18	4	-	-	43	6
Wherry:										
1001	-	-	16	5	-2	-	30	5	50	5
1011	-	-	13	5	-	-	6	5	17	6
MCA:										
578	87	8	-	-	43	10	-	-	-	-
343	50	5	28	5	15	5	-	-	11	3
21	-	-	18	9	-	-	-	-	-	-
Masonry:										
22	-	-	-	-	30	8	-	-	-	-
46	46	10	-	-	41	6	-	-	-	-
Ave % SD	47		19		29		18		26	

test holes or from the information in the as-built drawings. There is no clear-cut, single factor causing deviations. Orientation might be expected to be the biggest factor between northerly and southerly exposures. In fact, the southerly exposures appear to have had the biggest heat losses (the lowest R-values compared with expected).

Convection

The measurements of a given wall rendered R-values that varied on the order of 30% from the mean for that wall. This might be due to experimental variation or to varying thermal conditions. In building 21, pairs of sensors collocated at three locations resulted in variations of 2%, 0% and 26% of the average of the two R-values from the sensors. From these three instances one might expect variations of 10% around the average reading at a given site.

Table 8 demonstrates that the standard deviation is, on the average, three times greater than the variation obtained by replicating measurements at a given site. This implies that the thermal behavior of the structure is more variable than the instrumentation technique.

Plots of the percentage difference between the measured R-value of a point on a wall and the average R-value for all points on that wall reveal systematic patterns (Fig. 10). Figure 10a represents Wherry housing, which has no insulation in the wood frame construction. In this instance, convection is likely to occur. The graph bears out this likelihood, with higher apparent R-values at the top of a stud space than at the bottom. (There are two rises because of the fire blocking at midheight.) Larger R-values result from higher temperatures within the stud space, permitting less heat flow through the indoor surface at that location.

Figure 10b represents the performance of building 578, which may have insulation. The most probable reason for the greater variation in percentage difference in this case is that the ΔT during this period of measurement was nearly twice that during the measurements represented in the top graph.

Figure 10c represents the performance of the two Capehart buildings. These are insulated with 2.5 in. of fiberglass. The shape of these curves is different from the previous two examples. The sensor sites midheight between the plates and the fire blocking exhibit higher R-values than the sites 6 in. from the framing. This could be attributable to lateral conduction, which would be more pronounced through wallboard and insulation than it would be through wallboard alone, where lateral conduction might be overshadowed by convection effects. These characteristic curves agree with data presented by Handegord and Hutcheon (1953). Their laboratory results indicate that when a wall

Table 7. Percentage deviation of measured R-value from expected R-value. The number of values making up the average %Dev is *n* for each orientation.

	Walls								*Roof*		
	North		*East*		*South*		*West*				
Building	*%Dev**	*n*	*%Dev*	*n*	*%Dev*	*n*	*%Dev*	*n*	*%Dev*	*n*	*Notes†*
Capehart:											
933	3	5	-	-	-15	5	-	-	3	8	1
160	- 1	5	-	-	- 7	4	-	-	- 6	6	2
Ave	2	10	-	-	-11	9	-	-	- 1	14	
Wherry:											
1001	-	-	12	5	-	-	18	5	- 8	5	3
1011	-	-	19	5	-	-	03	6	0	6	3
Ave	-	-	16	10	-	-	10	11	- 4	11	
MCA:											
578	-37	8	-	-	-32	10	-	-	-	-	4
343	-21	5	-32	5	-36	5	-	-	-28	3	2
21	-	-	- 8	17	-	-	-	-	-	-	1
Ave	-31	13	-14	22	-33	15	-	-	-28	3	
Masonry:											
22	-	-	-	-	-34	8	-	-	-	-	4
46	18	10	-	-	-18	6	-	-	-	-	4
Ave	18	10	-	-	-27	14	-	-	-	-	
Grand Ave	- 6		- 4		-26		10		- 5		

* %Dev = $(R_{meas} - R_{calc})\ 100\%/R_{calc}$.

† Notes:

1. Based on sample boreholes in the test building.
2. Based on sample boreholes in a similar building.
3. Sheathing layer conductivity has a major impact on assumed R-value.
4. As-built drawing is the only independent confirmation.

the results of a computer simulation reported in Flanders and Marshall (1983).

Measurement validity

A constant sensor calibration in different environments is an important question affecting accuracy. Convection and other nonperpendicular heat flow paths add the question of consistency.

Sensor accuracy

Schwerdtfeger (1970) outlined how the sensor output depends on the thermal conductivity of the surrounding materials. In the Capehart, Wherry and MCA buildings the interior material was gypsum wallboard. The sensors were calibrated for this medium. However, plaster with a sand aggregate has 5 times the thermal conductivity of gypsum wallboard and concrete more than 11 times. This has a potentially significant effect on the validity of the calibration constant of the HFS.

Schwerdtfeger's analysis pertains only to an HFS surrounded by a homogeneous medium, not to a surface-mounted HFS. In his analysis, one of our HFSs would pass approximately 0.85 times more heat than the surrounding gypsum wallboard. For plaster the attenuation would be 0.40 and for concrete 0.21. If we assume that the HFS is surrounded by a medium that has the average thermal resistivity of the air and the wall material (Appendix C), these numbers change to 0.82 (gypsum wallboard), 0.63 (plaster) and 0.60 (concrete). This analysis is not exact, unlike Schwerdtfeger's, but gives possible orders of magnitude of the effect of different materials. Finally, from the ratio of the attenuation for plaster or concrete to the attenuation for gypsum wallboard, we might expect heat flow readings to be 23% less (plaster) to 27% less (concrete) than the actual value when the sensor is calibrated for a sheetrock surface.

Unfortunately this does not explain the results obtained for the concrete and plaster walls. Lower apparent heat flows in eq 1 would result in higher R-values, which is the opposite effect than that observed in two of three expected results.

Table 7 summarized the percentage deviations of measured R-values from those expected from

Table 6. R-value measurements for two masonry buildings.

	Number of measurements	R-value (°F hr ft²/Btu) Calculated	Measured	% Deviation*
Building 22 (concrete)				
North-northwest wall	-	-	-	-
South-southwest wall	8	3.2	2.1	-34
All walls	8	3.2	2.1	-34
Building 46 (plaster)				
North-northwest wall	10	3.1	3.7	+18
South-southwest wall	6	3.1	2.6	-18
All walls	16	3.1	3.3	+ 6

* % Deviation = $(R_{meas} - R_{calc})\ 100\%/R_{calc}$.

a. Building 22 shows cool (dark) areas where webs occur or blocks are filled with concrete. The light patches are aluminum tape.

b. Building 46 shows faint signs of horizontal strapping.

Figure 9. Thermograms of inside surface of walls of masonry construction.

R-values from those expected on the SSW walls of both buildings are of similar sense and magnitude. The northerly wall of building 46, however, had a deviation of similar magnitude but opposite sense from the southerly wall. It apparently has better insulating qualities. The evidence from building 22 alone would indicate that the calibration of the sensors does not generalize to the concrete surface they were placed on, but the building 46 data suggest the results are consistent.

For the eight sensor sites on building 22 that were centered on the blocks, the mean R-value was 2.0 with a standard deviation of 30%. Other sensor sites were chosen at 1.5, 2.5, 3.0 and 6.0 in. from the block centerline. Thermography revealed that the webs occurred a third of the way in from the ends and at the ends, so the centerline sites were farthest from webs, and the other sites were on webs. The four readings obtained at the 1.5, 2.5 and 2.0 in. stations represent a 3% increase in R-values over the center average, with a standard deviation of 14% of the mean. The three measurements obtained at 6 in. represent a 3% decrease, again with a standard deviation of 14% of the mean. Neither case is significantly different from the average at the center. This is consistent with

Table 5. R-value measurements for three MCA buildings assumed to have insulation in the walls. Building 578 is assumed to have 2 in. of fiberglass. Based on borings, buildings 343 and 21 have 3½ in. of fiberglass.

	Number of measurements	R-value (°F hr ft²/Btu) Calculated	Measured	% Deviation*
Building 578				
North wall	8	9.92	6.03	−37
South wall	10	9.92	6.53	−32
All walls	18	9.92	6.31	−34
Building 343				
North wall	5	14.0	11.0	−21
East wall	5	14.0	9.51	−32
South wall	5	14.0	8.93	−36
All walls	15	14.0	9.81	−30
Building 21				
East wall	17	14.4	13.3	− 8
All walls	17	14.4	13.3	− 8

* % Deviation = $(R_{meas} - R_{calc})\ 100\%/R_{calc}$.

When analyzed under the assumption that the three buildings contained insulation (2 in. for building 578 and 3.5 in. for buildings 343 and 21; Table 5), the measurements make more sense for buildings 343 and 21. The discrepancy between measured and expected values indicates that the actual performance is 30% and 8% worse than assumed for these two cases. The estimate for 578 is as far below expections now as it was above expectations under the assumption that the walls contained no insulation.

These measurements are as believable as the ones for the frame structures. The HFS was mounted on sheetrock in each instance, so that thermal environment remained equivalent. According to Madding (1979) the absorptivities of the brick on the outside of these buildings should not be appreciably different from the paint found on the frame buildings or from the masking tape employed to blend the solar radiation sensitivity of the outdoor temperature sensor to that of its surroundings. This construction incorporates vertical air spaces that probably result in convective currents. However, this did not constitute a problem for the measurements of Wherry housing, where vertical rows of sensors on walls accounted for the effects of convection. Building 343 had a forced hot-air heating system with outlets near the ceiling. This caused the data to fluctuate significantly near the ceiling but had no effect on the speed of convergence of eq 1 or its final R-value compared with lower locations.

Masonry buildings

The concrete block and colonial brick buildings represent both different construction and different measurement regimes for the sensors. The concrete block of building 22 has a surface thermal conductivity 11 times greater than the gypsum wallboard that was the surface material for the heat flow sensors in most of our measurements. The plaster interior of the building 46, the colonial, has a thermal conductivity 4.5 times that of the gypsum wallboard at other sites. The concrete block also contains thermal differences where webs conduct heat across the block more readily than where cores exist and where air convection currents are possible in a vertical direction within cores or between layers of blocks (Fig. 9). Building 46 showed some evidence of horizontal furring (Fig. 9); otherwise there was less thermal inconsistency near the interior surface.

Buildings 22 and 46 were measured during 23 February to 2 March and 4–8 March 1982, respectively. The sensors on building 22 were on a wall facing 204° on the true compass. Building 46's sensors were on walls facing 24° and 204°. Daily maximum ΔTs increased from 23° to 29°F in the first case and decreased from 18° to 14°F in the second. Skies were mostly clear when building 22 was measured and mostly cloudy when building 46 was measured. Winds were out of the north at less than 10 mph for both buildings.

The results for these two buildings are shown in Table 6. The percentage deviation of the measured

spaces. In this case the appropriate calculated R-value depends on whether the sheathing is fibrous cellulose insulating board or plywood. In the first case the R-value would be 3.6; in the latter case, 2.9. The following analyses assume plywood sheathing.

Two Wherry buildings were measured. Building 1001 (No. 14 Goodblood) had sensors during 17–22 February 1982. It faces 133° on the true compass. The maximum ΔTs for building 1001 were about 45–64 °F during the measurement period. Building 1011 (No. 68 Goodblood) was surveyed during 30 March–5 April 1982. It faces 311° on the true compass. The maximum ΔTs for building 1011 were about 20–32 °F during the measurement period. Sky cover during the two measurements was similar, but the wind was primarily out of the north in the first instance and out of the south in the latter.

The results (Table 3) from the two Wherry buildings were similar. The R-values of the two buildings differed by only 5% for walls and 9% for full-depth attic insulation. Again, the measured insulative value was higher than the value assumed. Had the assumption incorporated cellulose fiberboard sheathing instead of plywood, the wall measurements would have averaged 8% below the assumed R-value.

Again, the technique appears to be repeatable for two similar buildings with different temperature histories during measurement. The R-values are so small for the walls that a difference in any one element can have a major impact on the overall figure. The change in weather does not appear to have affected the role of the convective air within the uninsulated wall appreciably.

Frame and masonry buildings

According to their as-built drawings, MCA buildings may or may not have insulation within the frame structure, which has a brick veneer outside. The brick layer adds thermal inertia to the system and has the potential to smooth out the temperature extremes.

Two MCA buildings (578 and 343, apartment A in each case), with no insulation apparent in the as-built drawings, were measured during 2–8 February and 9–15 March 1982. The front entrances to these buildings face 81° and 46° on the true compass, respectively. Daily maximum ΔTs increased from 36° to 58 °F in the first case and decreased from 43° to 22 °F in the second. Sky cover and winds were similar for the two periods.

The results (Table 4) for these two buildings were very dissimilar. Building 343 registered R-values 1.5 times higher than those of building 578. These results are much higher than would be predicted from the assumption that there is no wall insulation. Thermography of building 578 indicated the presence of insulation (Fig. 5), with light stud spaces and dark studs. Figure 5 also indicates significant convective activity. Borings into the walls of a building identical to 343 revealed 3.5 in. of fiberglass insulation.

The third MCA example studied (building 21, room 11) contains 2 in. of insulation in the walls, according to the as-built drawings. Otherwise, the drawings showed the wall construction to be virtually identical to buildings 578 and 343. However, borings indicated 3.5 in. of fiberglass here, too. The weather was similar to when the other two buildings were measured.

Table 4. R-value measurements for two MCA buildings assumed from as-built drawings to have no insulation in the walls.

	Number of measurements	*R-value (°F hr ft²/Btu)*		*% Deviation**
		Calculated	*Measured*	
Building 578				
North wall	8	4.18	5.06	+ 21
South wall	10	4.18	6.82	+ 63
All walls	18	4.18	6.04	+ 44
Building 343				
North wall	5	4.18	10.8	+158
East wall	5	4.18	9.09	+118
South wall	5	4.18	8.52	+104
All walls	15	4.18	9.47	+127
Roof	3	14.6	10.2	− 30

* % Deviation = $(R_{meas} - R_{calc})\ 100\%/R_{calc}$.

Table 2. R-value measurements for two Capehart buildings.

	Number of measurements	R-value (°F hr ft²/Btu) Calculated	Measured	% Deviation*
Building 933				
North wall	5	9.77	10.1	+ 3
South wall	5	9.77	8.29	−15
Both walls	10	9.77	9.20	− 6
Ceiling	8	12.8	12.8	+ 2
Building 160				
North wall	5	9.66	9.77	− 1
South wall	4	9.09	9.77	− 7
Both walls	9	9.43	9.77	− 4
Ceiling	6	17.6	18.8	− 6

* % Deviation = $(R_{meas} - R_{calc})\ 100\%/R_{calc}$.

Table 3. R-value measurements for two Wherry buildings.

	Number of measurements	R-value (°F hr ft²/Btu) Calculated	Measured	% Deviation*
Building 1001				
West wall	5	2.87	3.41	+18
East wall	5	2.87	3.24	+12
Both walls	10	2.87	3.32	+15
Ceiling	8	21.0	19.3	− 8
Building 1011				
West wall	6	2.87	2.96	+ 3
East wall	5	2.87	3.41	+19
Both walls	11	2.87	3.18	+11
Ceiling	6	21.0	21.0	0

* % Deviation = $(R_{meas} - R_{calc})\ 100\%/R_{calc}$.

space and 2.5 in. of fiberglass insulation. Exterior inspection and as-built drawings indicated a single layer of textured plywood sheathing.

Two Capehart buildings (933 and 160, apartment C in each case) were measured during the periods of 9–16 February and 22–29 March 1982, respectively. The maximum ΔTs were 63 °F for building 933 and 43 °F for building 160. Building 933 faces 151° on the true compass, and 160 faces 155°. The sky cover, wind direction and wind speeds (Appendix B) were similar. Therefore, ΔT and possible differences in construction between two similar buildings were the only significant variables that might produce different results in the measurements.

The results (Table 2) from the two Capehart buildings were similar except for the insulation in the attic space above the upstairs ceilings. Appendix E contains sample time series data for ΔT, Q and R. The measurement technique is only expected to be valid for two significant figures. R-values of the north and south walls differed by only 0.57. On the average they were less than the expected value by 5%. The attic insulation measurements differed from the expected value by 2% and -6%.

The results show that the technique is repeatable. The tendency for measured values to differ from those calculated from handbook figures probably reflects actual conditions. Because the deviation is most pronounced on the south side of the building, the effect is probably due to the sun affecting the outdoor temperature sensors differently than the wall.

The Wherry wall has no insulation in the stud

earlier, the maximum potential deviation for a 24-hr cycle (Flanders 1980). This permits the investigator to determine how rapidly R_c is converging on a steady value. The purpose of this test is to permit the measurement to continue long enough to obtain convergence within a tolerance of the investigator's choosing without requiring unnecessary further measurement. Measurements at Ft. Devens lasted about 7 days per location in order to gain a variety of data for each location.

Thermographic mapping

Because no buildings demonstrated random variation in thermal properties, a thermographic map was made of only one wall at building 22. At about 0500 on 23 February 1982 a thermal survey of the south wall of the concrete block building commenced. The equipment included an Inframetrics Model 525 IR camera, with a video tape recorder connected to record both an IR and a video image (Fig. 7).

The survey involved setting up the camera at two distances, approximately 40 and 65 ft from the face of the wall, and panning to record details. This phase of the survey provided exploratory data for a future determination of what tradeoffs are necessary between resolution at close range and comprehensive coverage within one frame of view.

CASE STUDY RESULTS

One important purpose of the field investigation was to determine the reliability of the measurement apparatus. As-built drawings do not represent a reliable guide for how much insulation a wall contains or whether the sheathing is plywood or fiberboard. Measurements of at least two examples of the same type of construction at different times gave an indication of repeatability, and checking the results with assumed values from boring into walls and probing attic insulation gave a general idea about measurement reliability.

Frame buildings

The Capehart and Wherry frame buildings represent structures with and without some insulation. The thermograms in Figure 8 confirm that the insulated stud spaces in the Capehart structure retain heat better than the stud locations; the reverse is true in the Wherry structure.

The as-built drawings (Fig. 2) for Capehart construction indicate 2 in. of fiberglass batt insulation in a 3.5-in. stud space. This renders an estimated thermal resistance of $R = 8.2$. If the stud space were completely full of fiberglass insulation, then the R-value would be 13. A $\frac{1}{8}$-in. inspection hole drilled at two places in building 933 revealed a 1-in. double layer of gypsum wallboard, a 1-in. air

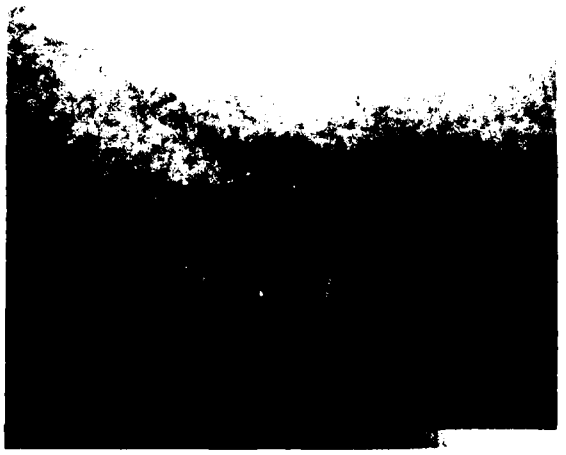

a. Capehart. The studs are cooler (darker) than the better-insulated stud spaces.

b. Wherry. The stud spaces are uninsulated and show as cooler than the studs. Plastic electrical plugs and wires are visible, but the masked area on the sensor is not.

Figure 8. Thermograms of interior views of walls of frame buildings. Light shades indicate warm surfaces.

least in the spectral window of the IR camera. If the material—masking tape in this case—is invisible to the camera, then the match is good.

Heat flow sensors were taped to indoor surfaces without any "gooey" material at the interface. Flanders and Marshall (1983) determined that on a reasonably smooth surface like polystyrene or gypsum wallboard, there was no significant benefit to be gained from petroleum jelly or heat conduction grease. Johannesson (1979) indicated that an air gap of 0.02 in. or smaller between an HFS and the measured surface will have an inconsequential effect on measurement accuracy.

Thermocouple installation on the exterior also utilized masking tape as a radiation guard (see cover). Outside, the tape extended about 1 ft along the length of the wire from the end to establish contact with the building surface and to diminish the potential for radiation heating the wire insulation more than the building surface.

Data acquisition

The 20 sets of two thermocouples and one heat flow sensor provided the input to a Hewlett Packard 3497A Data Acquisition System (DAS), whose specifications are in Appendix A. This device controlled the input in sequence, digitized it and passed it along to an Apple II Plus computer. The computer controlled when the DAS read the sensor signal, logged time series data on a flexible diskette, kept a running computation of the calculated R-value for each data site, and displayed the status of the measurements on a video monitor.

The time series data included indoor and outdoor surface temperatures and heat flux for each sensor site, recorded at 20-minute intervals. Readings from each sensor occurred about once every 40 seconds, and these were averaged until they were recorded on the disk. A backup file on the disk stored the status of the essential variables in case of a power failure. The system could thereby restart automatically and decide whether to continue the previous measurement series after a brief interruption or start a new series. A printer recorded the essential results on an hourly basis to further back up the disk system. The controlling data acquisition program (DAP) is described and listed in Appendix A.

The DAP estimates the R-value according to the formula

$$R_e = \frac{\Sigma \Delta T_i}{\Sigma Q_i} \qquad (1)$$

where R_e = estimated R-value
ΔT_i = difference in temperature across the structure at the ith reading
Q_i = heat flow at the ith reading.

Equation 1 represents the ratio between the accumulated differences in temperature across the structure and the accumulated heat flows through it. Because of the lag between a temperature potential across the structure and the resulting heat flow through the structure, eq 1 only approximates the R-value obtained under steady state temperature and heat flow in a laboratory test. The longer the duration of measurement, the closer the value of R_e approximates the true R-value. This formula is widely used and is derived in Flanders and Marshall (1983).

The DAP also records the fractional deviation of the current value of R_e from the value of 6 hrs

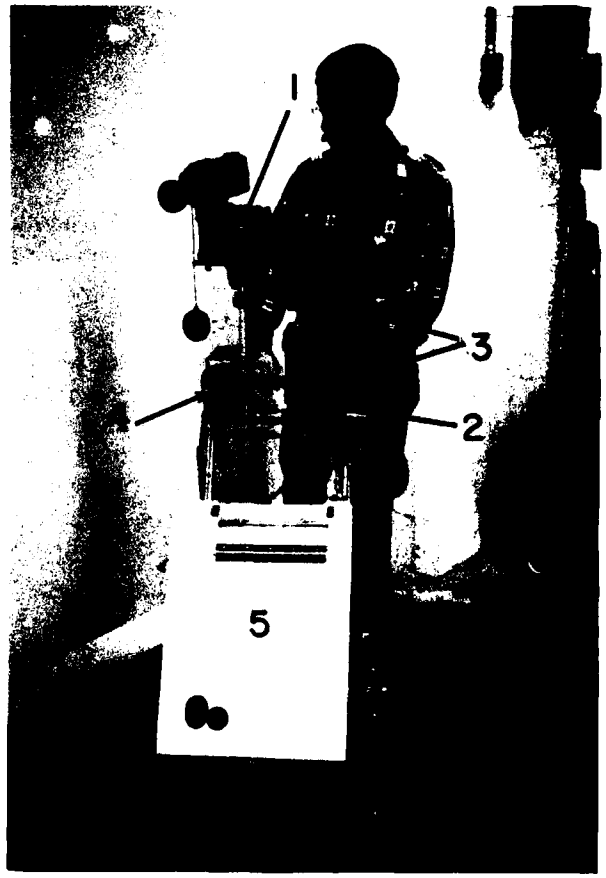

Figure 7. Thermography apparatus used at Ft. Devens: imaging sensor (1), control unit (2), monitoring screen with Polaroid camera (3), power supply (4) and video recorder in an insulated box (5).

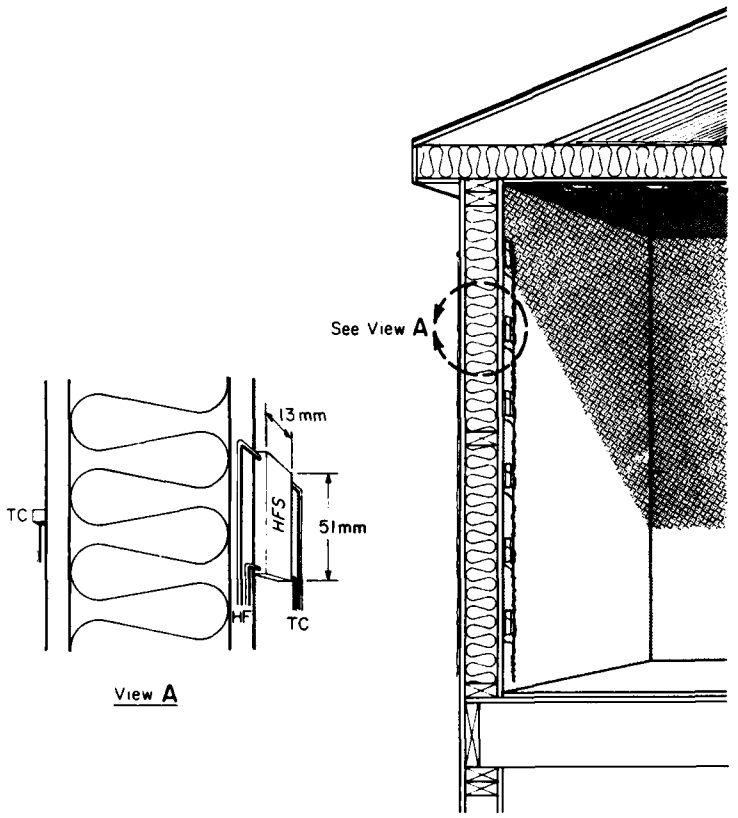

Figure 6. Overall placement of temperature sensors on inside and outside surfaces and an HFS inside.

Studs were not chosen as sensor sites because the potential for unpredictable thermal performance is small at such sites. A stud site might serve as a location for confirming the validity of measurements elsewhere, except that heat flow tends not to be perpendicular to the plane of the wall there. Consequently, interpretation of the results might be unreliable.

Emplacing thermal sensors

Each sensor site hosted two temperature sensors, one each on the inside and outside surfaces, and a heat flow sensor on the inside surface (Fig. 6). Thermocouples sensed temperature, and thermocouple-based thermopiles constituted the heat flow sensors (HFSs). Thermocouples for exterior use were simply copper and constantan wires twisted together and soldered in contact with each other. Indoor thermocouples were integral to the HFSs.

The HFSs were 0.5- by 2.0-in. rectangular wafers 0.1 in. thick, containing the coils of wire wrapped around a 0.3- by 1.5-in. core about 0.05 in. thick. The HFS nominal sensitivity was approximately 7–10 Btu/ft²•hr•mV. The sensor's millivolt output is the sum of the temperature differences between each successive junction on either side of the core material for the coil. This sum is directly related to the heat flowing through the intervening core thickness between the junctions within the HFS.

Ideally heat flow sensors and temperature sensors should be buried in the structure, with just a thin layer of the surrounding material covering the site. In this way the sensor might "feel" exactly the thermal stimuli that the structure experiences. However, the survey procedure required that the measured surface be unblemished and that the sensors be retrievable for the next measurement. Therefore masking tape completely covered all sensors when in place.

Masking tape, like most nonmetallic materials, has an absorptance of about 0.9 and therefore blends with its surroundings in its ability to absorb thermal radiation. Infrared thermography can confirm the efficiency of this blending effect, at

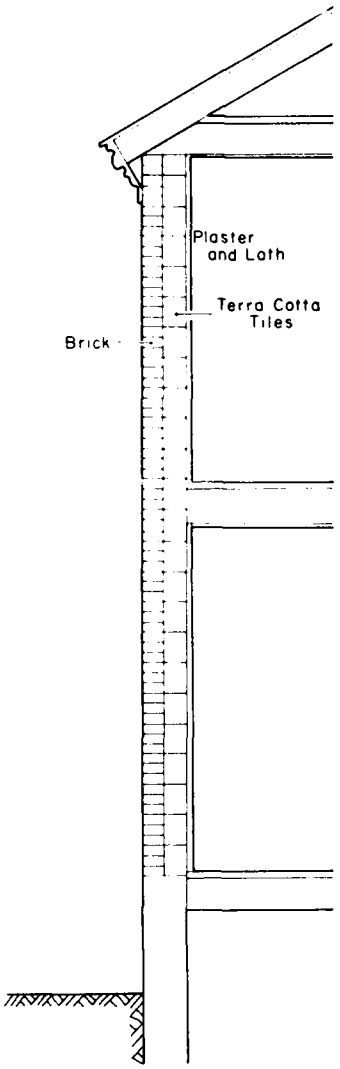

b. Colonial brick building.

Figure 4 (cont'd). Typical cross sections of masonry buildings at Ft. Devens, according to as-built drawings.

Figure 5. Thermogram of convection cells in stud spaces. The light areas are warmer than the dark areas. Vertical studs and horizontal blocking at midheight are visible.

Case study measurement procedure

The measurement procedure entailed four steps: 1) establishing sensor sites with infrared thermography, 2) emplacing thermal sensors, 3) recording the sensor's responses to temperature and heat flow changes in the structure, and 4) mapping the region of measurement thermographically. The last step was omitted if step 1 located no anomalies; predictable thermal discontinuities, like studs, also did not warrant step 4.

Establishing sensor sites

Infrared thermography determined the strategy for locating sensors. In frame walls there was seldom evidence of random thermal anomalies. Almost always the vertical studs and the horizontal fire blocking at midheight were evident. Often convection in the stud space (Fig. 5) was visible as regions at the top of a space that were lighter (warmer) than at the bottom. Therefore, sensors were placed along a vertical line midway between joists (Fig. 6 and cover), typically three above the fire blocking and three below. This practice is also consistent with the observations and recommendations of Handegord and Hutcheon (1953). Had there been a surface with random thermal anomalies, sensors would have been placed at the apparent thermal extremes and at locations of intermediate thermal qualities. In one case the concrete block wall, the web within blocks, and the vertical air spaces in the cores and in the spaces between layers constituted known thermal dissimilarities.

The objective is to characterize the thermal performance of all similarly insulated surfaces from a small sample. Thermography revealed the consistency among stud spaces. Sensor sites on the northern and southern exposures of the building provided maximum potential variation in thermal performance. In the frame buildings surveyed, this should be sufficient representation of the whole.

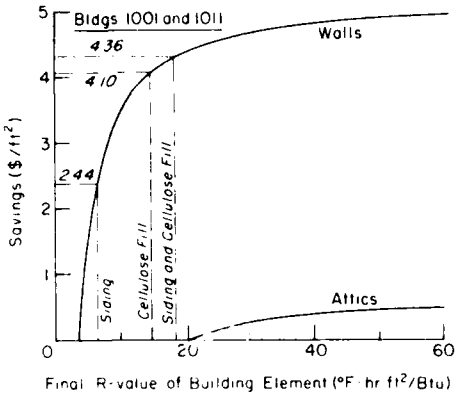

Figure 14. Fifteen-year present worth energy savings potential for adding insulation to two Wherry family housing buildings as a function of the final R-value.

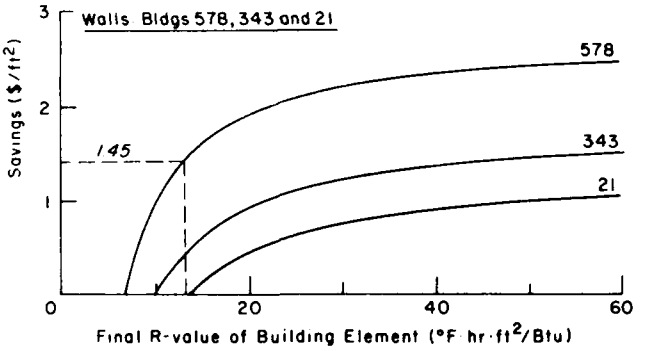

Figure 15. Fifteen-year present worth energy savings potential for adding insulation to three MCA buildings as a function of the final R-value. The dashed line is the estimated cost of installing a stucco-beadboard polystyrene insulation system on building 578.

Savings potential in MCA buildings

The MCA buildings have a moderate potential for thermal improvement (Fig. 15). Since these buildings have a durable brick exterior, an exterior insulation project would be difficult to justify esthetically or on grounds of durability of cladding. Building 578 would warrant spending $1.45/ft² (15 years) to blow in insulation to bring it up to an R-13.

The one MCA building roof we measured was a cathedral system with a sloped built-up roofing system. Unless the roof is due for replacement, it is difficult to justify adding insulation on the outside. Adding insulation to the inside would require furring, gypsum wallboard and finishing.

Savings potential in masonry buildings

The measurement results for the two masonry buildings show significant potential for thermal improvement (Fig. 16). The estimated insulation costs are based on data obtained from manufacturer's representatives for a plastic foam exterior insulation system with a reinforced stucco finish. They represent $4.10/ft² for installation of the stucco-finish system and $0.30/ft² for each inch of expanded polystyrene at R-3.6 per inch. Where the building "budget" curve is higher than the insulation cost line at a vertical slice through the graph, a cost savings occurs for each final R-value on the horizontal axis. The ratio between the cost and the savings shown at each vertical slice through the

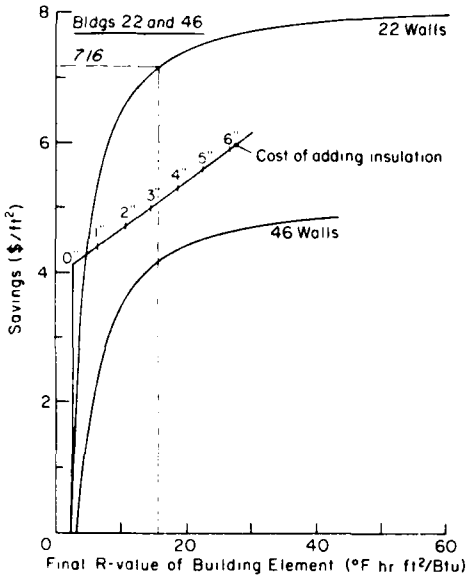

Figure 16. Fifteen-year present worth energy savings potential for adding insulation to two masonry buildings as a function of the final R-value. The dashed line is the estimated cost of installing a stucco-beadboard polystyrene insulation system on building 22.

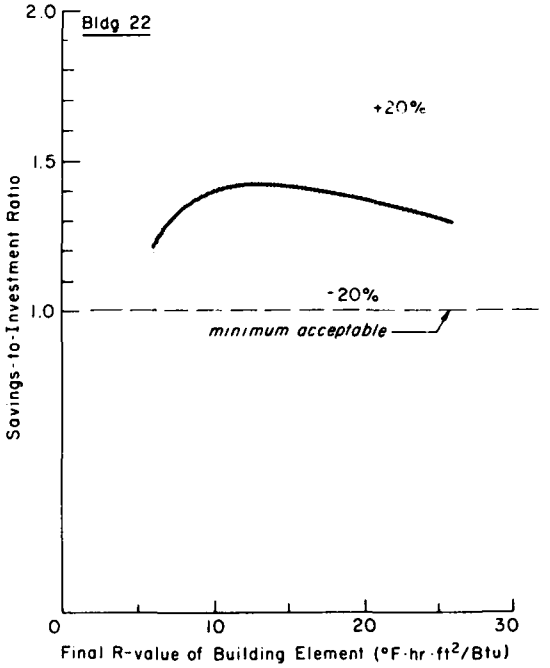

Figure 17. SIR for employing stucco-beadboard polystyrene exterior insulation on building 22 as a function of the resulting R-value. The shading depicts how the SIRs would change with a 20% variation in the assumed savings.

graph is the SIR; when SIR ≥ 1, the project saves money.

The SIR for building 22 ranges between 1.2 for 1 in. of polystyrene to a maximum of 1.4 near 3 in. of insulation, tapering to 1.3 at 6 in. of insulation (Fig. 17). From the point of view of life-cycle costs, these thicknesses are similar. One would choose the least insulation thickness to minimize first cost, the greatest thickness to maximize energy savings, or the maximum SIR to have the best shot at competing with other ECIP projects.

The maximum SIR occurs at a point where the slope of the "budget" curves equals the slope of the cost line. The first derivative of eq 4, where $R = 1/U$, is

$$\frac{dS}{dR} = (\mathrm{CHC})(R^2) \qquad (5)$$

$$= \frac{dD}{dR}$$

where C is the cost of insulation. Solving eq 5 for R, we obtain the "optimum," where

$$R = [(\mathrm{CHC})/(dC/dR)]^{1/2} \qquad (6)$$

which, for the data in Figure 16, is $R = 15.3$. Thus, insulation costing \$7.16/ft² would still yield an SIR of 1 over 15 years.

A heat-exchanger ventilation system and new, tighter windows would improve the building's energy-efficiency further. The added insulation would then cause the building to perform more like a super-insulated building and would not bend the SIR curves downward as much as the R-value becomes higher.

The concrete block construction lends itself well to an exterior insulation system, since the improvement in esthetics would be significant. Furthermore, the impregnated pigment of the stucco would eliminate the need for repainting, which is a chronic problem with concrete block buildings.

Building 46 (Fig. 16) has a significant energy conservation budget, but it is not high enough to justify the exterior insulation system. With no cavities to fill, it is architecturally difficult to devise an insulation system that would be economical and meet code. A layer of foam insulation covered with gypsum wallboard applied to the interior might be feasible.

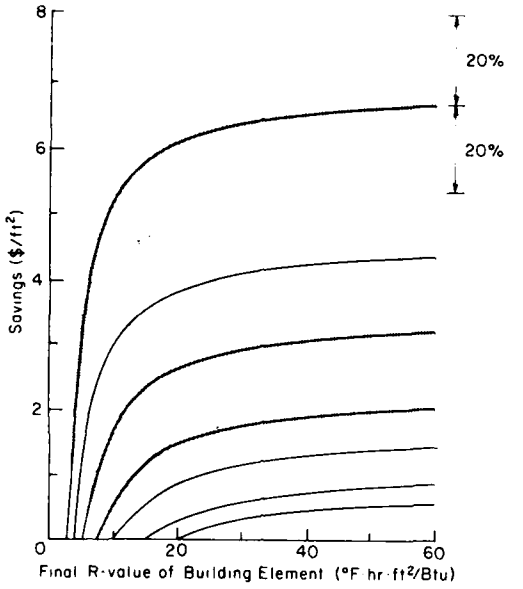

Figure 18. Fifteen-year energy savings potential for any building at Ft. Devens. The initial R-value is where a line intercepts the horizontal axis.

Sensitivity of the analysis

Many factors have a potential impact on the accuracy of the savings analysis: the assumed impact of internal heat loads, the heating plant efficiency, the actual rate of fuel cost inflation, and the maintenance costs of heating plants are major factors. Figure 18 depicts the general case for which Figures 13-16 are examples. It shows that for Ft. Devens, marginal improvements in R-value beyond 15 °F hr ft²/Btu result in small additional savings. The shaded areas demonstrate the impact of overestimating or underestimating the CHC by 20%. Such an error probably would not change the conclusions reached in the preceding discussion.

CONCLUSIONS

This report describes

1) The reliability of a technique for measuring building envelope thermal performance in situ.

2) The thermal health of buildings at Ft. Devens.

3) The economic potential for investment in improved insulation at Ft. Devens.

The results of this pilot study indicate that, for Army construction at least, the measurement technique results in few surprises in calculating R-value. The Ft. Devens buildings also contain no surprises in the thermal status or investment potential. A follow-up report is planned, based on additional data from Fort Carson, Colorado, and Fort Richardson, Alaska, which will expand the scope of inquiry to the benefits of building mass, for which ordinary hand calculation techniques are inadequate and for which field measurements may provide essential information.

Measurement reliability

The case study results demonstrated that for similar types of construction under different weather regimes the repeatability of the measurement was good. For Capehart insulated frame buildings the wall measurements did not vary. For the Wherry uninsulated frame buildings the wall measurements differed by 5% between two buildings. Convection under differing weather conditions may partly explain this latter difference. The R-values were also believable, although they differed from the expected value by as much as 15% where the construction was verified by boring and 37% where the construction was assumed to be similar to that where a boring was obtained.

The calibration and sensitivity results showed that the sensors were insensitive to the difference in surface conductivity between gypsum wallboard and extruded polystyrene insulation board. A 30% difference was expected. A similar difference was expected between wallboard and concrete but was not tested.

Thermal status of Army buildings

The preliminary thermographic overview of buildings at Ft. Devens indicated an overall consistency of thermal performance between buildings of like construction. Therefore, a sampling of buildings should suffice to characterize the thermal status of all similar buildings. We detected no evidence of failed vapor barriers, missing insulation or other possible major failings and faults.

Economic potential for investment in insulation

The case study results indicate that the investment potential for increased insulation in the types of buildings surveyed at Ft. Devens is as follows:

Capehart:	Walls - $0.50/ft² to add R-3.6 at SIR = 1
	Attics - 4 in. more at a low SIR
Wherry:	Walls - possible SIR = 3.3 to fill
	Attics - no potential
MCA:	Walls - poor potential
	Attics - insufficient data

Masonry block: Walls - possible SIR = 1.4 for an external foam/stucco system
Attics - no data
Colonial: Walls - consider foam insulation and gypsum wallboard applied to interior surface of walls
Attics - no data.

The buildings with the most clear-cut potential for thermal improvement are the masonry block construction. For these, an exterior stucco-on-polystyrene insulating system offers good potential. For the Wherry and colonial buildings there are some construction and esthetic issures. These recommendations are all preliminary and warrant more detailed examination before deciding on an insulation project.

LITERATURE CITED

ASHRAE (1977) *Handbook of Fundamentals.* New York: American Society of Heating, Refrigerating and Air Conditioning Engineers.

ASTM (1984) *Annual Book of ASTM Standards. Part 18. Thermal and Cryogenic Insulating Materials; Building Seals and Sealants; Fire Standards; Building Constructions; Environmental Acoustics.* Philadelphia: American Society for Testing and Materials.

Dow (1976) Styrofoam building insulation properties and limitations. Dow Chemical Corp., Form No.179-4108-76.

ECIP (1982) Energy Conservation Investment Program Guidance. Department of the Army letter from AFEN-RMR CHQ FORSCOM, Ft. McPherson, Georgia, 13 October.

Flanders, S.N. (1980) Time constraints on measuring building R-values. USA Cold Regions Research and Engineering Laboratory, CRREL Report 80-15.

Flanders, S.N. (1982) Least life-cycle costs for insulation in Alaska. USA Cold Regions Research and Engineering Laboratory, CRREL Report 82-27.

Flanders, S.N. and S.J. Marshall (1984) Toward in-situ building R-value measurement. USA Cold Regions Research and Engineering Laboratory, CRREL Report 84-1.

Handegord, G.O and N.B. Hutcheon (1953) Thermal performance of frame walls—Air spaces blocked at mid-height. Division of Building Research, Ottawa, Canada, Research Paper No. 10.

Korhonen, C. and W. Tobiasson (1978) Detecting wet roof insulation with a hand-held infrared camera. *Proceedings of the Fourth Biennial Infrared Information Exchange.* IRIE. Reprinted as USA Cold Regions Research and Engineering Laboratory, CRREL MP 1213.

Johannesson, G. (1979) Heat-flow measurements: Thermoelectric meters, function, principles and sources of error. Lund Institute of Technology, Lund, Sweden, Report NBH-3003. (English draft translation available through CRREL).

Madding, R.P. (1979) Thermographic instruments and systems. University of Wisconsin, Madison.

Reynolds, Smith and Hill (1981) Energy engineering analysis—Project evaluation: Insulation of temporary buildings, Ft. Devens. Reynolds, Smith and Hill, Architects-Engineers-Planners, Inc.

Schwerdtfeger, P. (1970) The measurement of heat flow in the ground and the theory of heat flux meters. USA Cold Regions Research and Engineering Laboratory, Technical Report 232.

APPENDIX A: SYSTEM SPECIFICATIONS

Data acquisition system

The system included a Hewlett-Packard 349A data acquisition/control unit with front panel and display, real-time clock and HPIB interface with the following installed options:

- 5½ digit, digital voltmeter (-001)
- 20-channel relay multiplexer, 1 each, (-010)
- 20-channel relay multiplexer with hardware type-T thermocouple compensation, 2 each, (-020-T20)
- 16-channel actuator/550 digital output assembly, 1 each, (-110)
- clock format (mo:day:hr:min:sec) (-230)
- 120 V, 60 Hz power (-326)

Computer controller

The controller of the HP 3497A was an Apple II Plus computer (A251048) with the following specifications and options:

- 48K bytes RAM with keyboard, power supply and ROM floating point BASIC interpreter
- 16-sector (DOS 3.3) drive for 5.5-in. floppy disks, 2 each, (A2M0044, A2M002)
- Silent thermal printer (A2M006)
- 9-in. B&W video monitor, 1 each, (A2M005)
- General Purpose Interface Bus (IEEE-488) from California Computer Systems, 1 each, (CSS 7490A)
- Micromodem with automatic dial-up and answering firmware on EOM from D.C. Haynes Assoc., Inc.

Data acquisition programs

The startup program initializes the data acquisition parameters and runs the data acquisition program.

The data acquisition program self-loads and runs when the computer is powered up in case of power failure. It collects data for 60 sensors every 40 seconds, averages the data, and writes it to a file at the interval specified in the startup program. Each write-to-disk has its own file name. The program provides an opportunity to interrupt data collection to inspect readings, change parameters, etc. Nevertheless, it will continue to read data at 120-second intervals.

Data transfer and analysis programs

An Apple program transfers the data via a modem to a main-frame computer. A program on the main-frame computer re-sorts the data into a separate time series for each sensor for ΔT, Q, R and convergence of R.

APPENDIX B: WEATHER DATA

Wind speed and direction, sky cover and precipitation data come from records obtained from Ft. Devens' airfield, located a short distance from the main post.

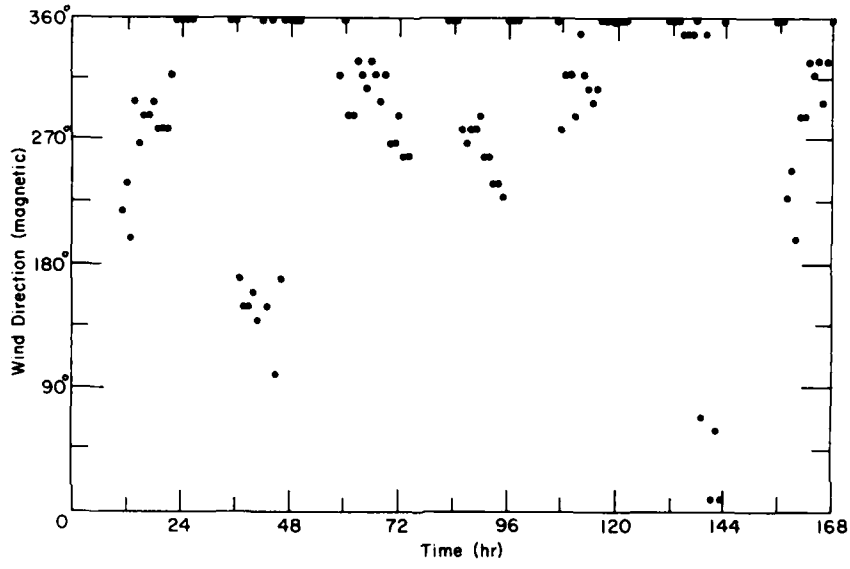

Figure B1. Hourly wind direction at Ft. Devens airfield during the thermal measurement period for building 933.

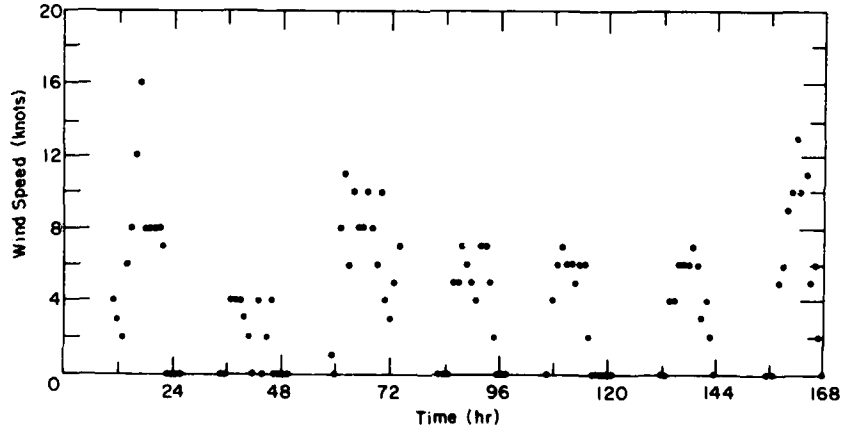

Figure B2. Hourly average wind speed at Ft. Devens airfield during the thermal measurement period for building 933.

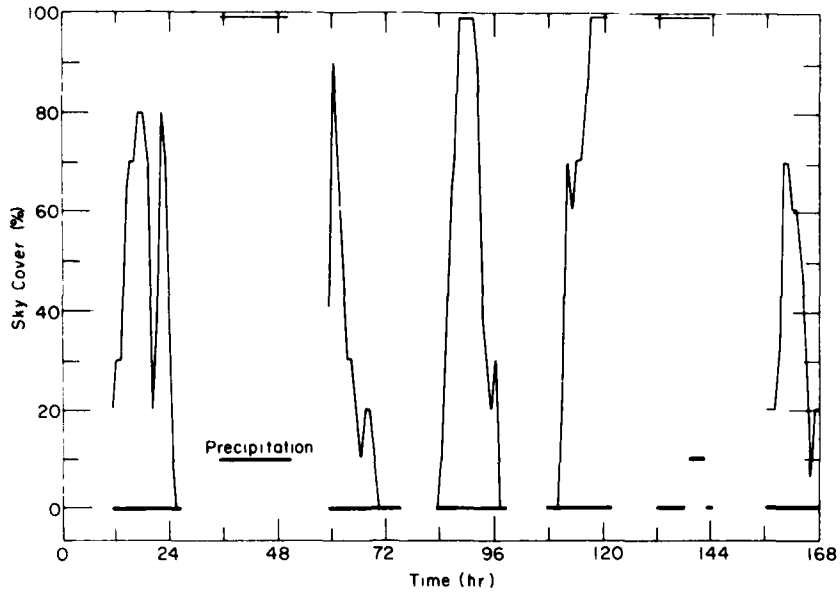

Figure B3. Sky cover and presence of precipitation during the thermal measurement period for building 933. Data were not obtained for night hours.

APPENDIX C: SENSOR SENSITIVITY TO SURROUNDING MATERIAL

Schwerdtfeger (1970) explained the potential sensitivity of HFS accuracy to the thermal conductivity of the surrounding materials. He described this accuracy in terms of Q_s/Q_m, where Q_s is the heat flow passing through the sensor and Q_m is that passing through the surrounding medium at a place undisturbed by the sensor. (This discussion employs different symbols than Schwerdtfeger used.) The sensitivity of Q_s/Q_m is a function of a geometric parameter G and K_s/K_m, where K_s is the thermal conductivity of the sensor materials and K_m is the thermal conductivity of the surrounding materials.

Figure C1 demonstrates that as the sensor becomes more conductive than the surrounding material, it tends to focus heat flow through it and act as a conduit. Conversely, when it becomes more resistive it tends to block heat flow. Figure C2 shows the resulting functional relationship: as the sensor becomes more of an impediment to heat flow, sensor readings increasingly underestimate heat flux.

In the case of the sensors I used at Ft. Devens, which were 0.5 × 2 × 0.08 in., the dimensionless geometric parameter was

$$G = \sqrt{A/2t} \qquad \text{(C)}$$

$$= 6.44$$

where A is the area and t is the thickness of the sensor.

If we assume the thermal conductivity of the sensor is 0.5 Btu in./hr ft² °F, then its sensitivity to surrounding homogeneous materials would be as shown in Table C1 for the materials I encountered in the field or in the laboratory.

However, Schwerdtfeger's analysis does not apply exactly to my measurements, where the HFS was mounted on a solid surface and was surrounded by air. To estimate the effect of this environment, we can combine the contributing effects of air and solid in one artificial K_m. Because a low-conductivity material controls the rate of heat flow in a serial system, Table C2 employs the average of the resistivities of air and the solid. K_m is the inverse of the average resistivity.

Table C2 indicates that the change of materials has an effect similar to that in Schwerdtfeger's an-

Table C1. Thermal conductivities (Btu in./hr ft² °F), conductivity ratios (for our sensor) and heat flow response (Q_s/Q_m from Fig. C2).

Material	K_m	K_s/K_m	Q_s/Q_m
Polystyrene	0.2	2.6	1.1
Gypsum wallboard	1.1	0.45	0.85
Plaster	5.0	0.10	0.40
Concrete	12.5	0.04	0.21

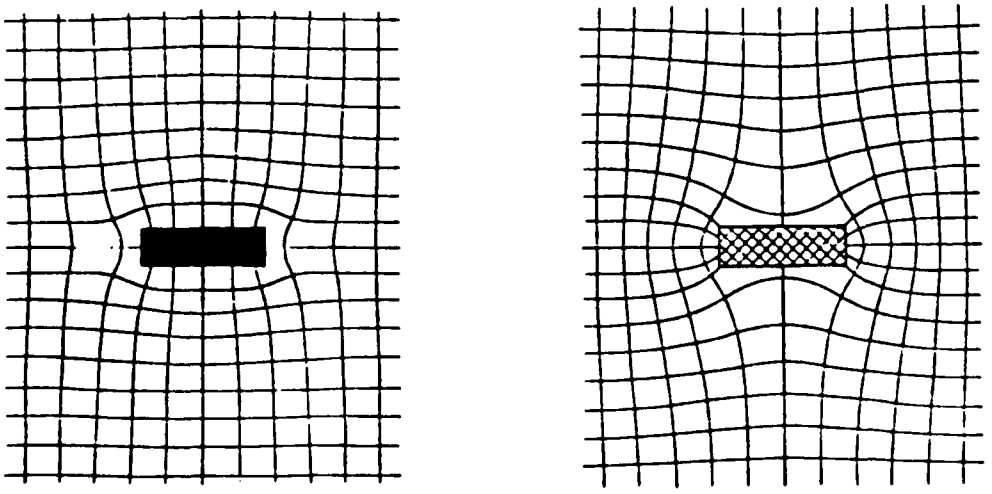

a. $K_s/K_m = \infty$. *b.* $K_s/K_m = 0$.

Figure C1. Simulated isotherms and lines of equal heat flow density. (From Schwerdtfeger 1970.)

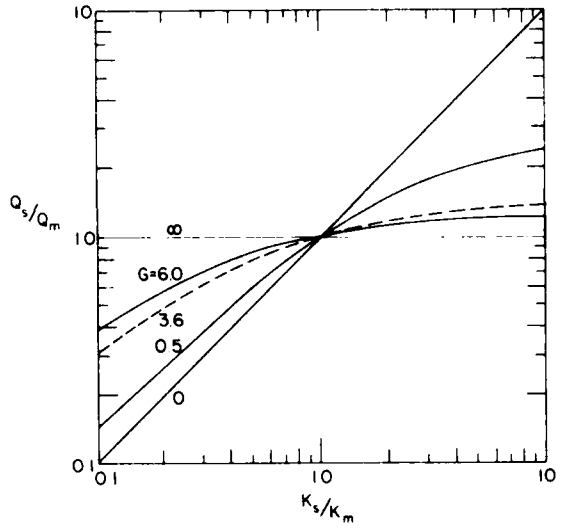

Figure C2. Normalized heat flux as a function of the conductivity ratio K_s/K_m for several values of the geometric parameter G. (After Schwerdtfeger 1970.)

Table C2. Thermal resistivity (hr ft² °F/Btu in.) of the solid material, an artificial K_m that combines the resistivities of air and the solid material, conductivity ratio and heat flow ratio. The resistivity of air is assumed to be 0.75.

Material	*1/K*	K_m*	K_s/K_m	Q_s/Q_m
Polystyrene	5.0	0.35	1.44	1.1
Gypsum wallboard	0.91	1.21	0.42	0.82
Plaster	0.20	2.11	0.24	0.63
Concrete	0.08	2.41	0.21	0.60

* $K_m = 2/(0.75 + 1/K)$

alysis for homogeneous surrounding material when the solid is about as conductive or more conductive than the HFS. If the solid is much more conductive, then the conductance of the air diminishes the tendency for the sensor to underestimate heat flux.

This estimate of sensitivity is still much greater than I encountered in the laboratory experiments outlined in Appendix D.

APPENDIX D: HFS CALIBRATION AND SENSITIVITY TESTS

I calibrated the HFSs I used at Ft. Devens in a large-scale calibrated hot box (Fig. D1). I also tested the sensitivity of these and other sensors in the same apparatus.

Calibration

The first three calibration runs took place on a vertical surface consisting of 2 in. of extruded polystyrene foam insulation and 0.5 in. of gypsum wallboard held against the insulation with springboards. This structure had an R-value of 10, according to data supplied by the manufacturer of the foam (Dow 1976), the results of guarded hot box tests (Greatorex 1982), and ASHRAE (1977). The second three runs employed the same structure minus the wallboard, with an R-value of 9.9 expected. Therefore, this construction would be expected to conduct heat at a rate 3% higher than with the wallboard. The order of these runs with

Figure D1. Calibrated hot box and moisture test facility used to calibrate the HFSs. A refrigerated chamber (1) and a heated chamber (2) maintain a constant temperature drop across a test wall held in a frame (3).

Table D1. Sensor location plan by test run sequence number. The location numbers are sequential from left to right and top to bottom in the 5 by 4 grid.

	Location no.																			
	1	*2*	*3*	*4*	*5*	*6*	*7*	*8*	*9*	*10*	*11*	*12*	*13*	*14*	*15*	*16*	*17*	*18*	*19*	*20*
Run	*Sensor no.*																			
1:	14	10	2	20	13	9	18	6	15	17	11	12	1	16	4	7	19	8	3	5
2:	19	20	1	11	9	15	7	16	3	8	2	17	5	12	14	6	4	18	10	13
3:	7	5	8	13	15	14	1	10	11	4	19	3	12	18	16	20	17	2	6	9
4:	15	11	16	4	8	17	2	7	10	18	20	12	1	19	9	13	14	3	6	5
5:	2	16	3	17	20	12	10	5	11	4	13	1	19	7	14	18	8	6	15	9
6:	11	1	9	14	2	4	12	20	7	3	13	8	19	16	5	18	17	15	10	6

and without wallboard was not randomized because the availability of the testing facilities was uncertain.

The test sensors were arranged on a five-horizontal by four-vertical intersection grid according to the randomized plan in Table D1. Each intersection was 8 in. apart horizontally and 9 in. apart vertically. The sensors were attached with masking tape covering the entire sensor and lapping onto the wall as was done in the field. The temperatures in the test apparatus were set at approximately 68 °F on the warm side and 14 °F on the cold side and were allowed to vary only by about 1% and 10%, respectively. The system was allowed to stabilize for at least 12 hr; then temperature and heat flux data were obtained every 40 s, averaged, and then recorded as an average on a floppy disk every 20 min, using the DAS described in Appendix A.

The calibration constants obtained from these runs were calculated according to eq 2. The average calibration constant for the three runs with foam was 2.7% higher than the average for the three on wallboard, with a standard deviation of 10.2% of the mean.

Sensitivity

A second set of experiments was designed to test the sensitivity of sensor calibration figures to their thermal environment. The test procedure was the same as for calibration, but the following variables were changed: three sensor types were used to determine the effect of sensor shape and construction; three means of covering the sensors included one with convective surroundings and two with conductive surroundings; and three wall materials represented two surface types—foam insulation and gypsum wallboard—and two levels of insulation. Table D2 summarizes the types of HFSs, the sensor treatments and the wall types used in the sensitivity experiment.

The sensitivity study included sensors used at Ft. Devens and two other types. The Ft. Devens HFSs were ITI model B'-329, constructed of a "Micarta"-like material and measuring 2 × 0.5 × 0.1 in. The Hycal LO-2 was a similar-sized HFS, except it was 0.1 in. thick and incorporated an aluminum layer on one side of a plastic layer containing the sensing coils. The third sensor was by Medtherm and was 3 × 4.38 × 0.1 in. of fiber-reinforced resin with a 1- × 1.5-in. sensing area in the center. The ITI sensors were calibrated as described above. The other two sensors were calibrated in an ASTM C518 heat flow meter apparatus, sandwiched between a layer of fiberglass insulation and neoprene foam with a "Micarta" guard surrounding the sensor.

Table D2. Experimental plan for HFS sensitivity tests.

			Condition		
Sensor type	*No.*	*Treatment*	*Run:* *1*	*2*	*3*
Hycal	1	P	H	L	G
	2	T	H	G	H
	3	G	G	H	L
	4	T	L	H	L
	20	T	G	L	G
ITI	5	T	H	G	L
	6	T	L	G	H
	7	T	L	H	G
	8	T	G	L	H
	14	P	H	H	L
	15	P	G	L	H
	16	P	L	G	G
	17	G	H	G	G
	18	G	L	L	L
	19	G	G	H	H
Medtherm	10	T	L	H	L
	11	T	H	G	H
	12	T	G	L	G
	13	T	H	GL	

Sensor cover material:
T = tape
P = plywood
G = gypsum wallboard

Wall material:
G = gypsum wallboard
H = polystyrene foam with a high R-value
L = polystyrene foam with a low R-value

The sensitivity experiments used the same two surface conditions as for calibration but added a layer of 1-in.-thick extruded polystyrene as another condition. These three conditions were set up permanently side by side throughout the series of three tests. Randomizing their position would have been desirable but too time consuming under the circumstances.

Three sensor treatments were tried. Masking tape over the HFS duplicated the technique used at Ft. Devens. Covers, 1 ft square, made from 0.5-in. plywood or 0.5-in. wallboard offered the potential for calibrating sensors in a smaller laboratory thermal testing machine. Furthermore, Schwerdtfeger's analysis would apply when a sensor is completely surrounded by wallboard.

The experimental plan was as outlined in Table D2. A sensor would be placed on either the wallboard surface (which had foam underneath), the

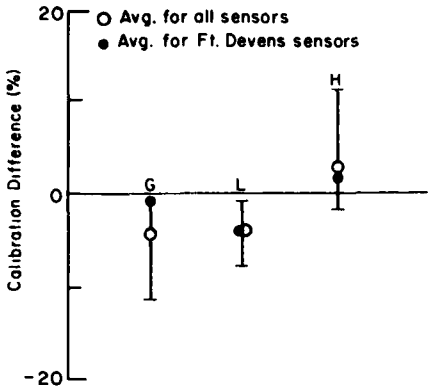

Figure D2. Average difference in sensitivity for each sensor and wall condition compared to an independent calibration, either from the large-scale calibrated hot box or from an ASTM C518 heat flow meter apparatus.

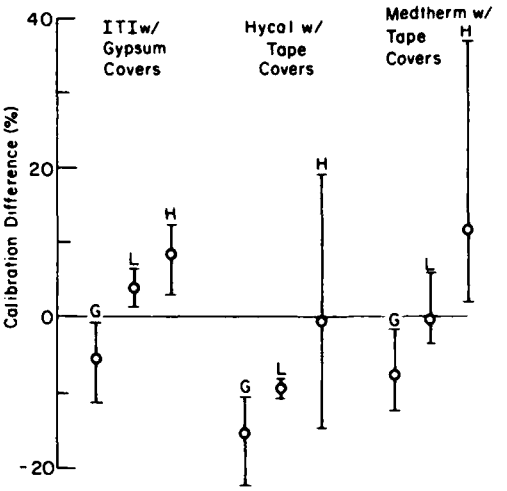

Figure D3. Effects of ITI sensors with gypsum wallboard covers relative to calibrated hot box calibration, Hycal sensors with tape covers relative to heat flow meter (HFM) calibration, and Medtherm sensors with tape covers relative to HFM.

standard polystyrene foam surface, or the foam with 1.5 times the thickness. Each surface condition had its own five-by-four intersection grid, as before. When the plan called for a sensor with its treatment to be on a given surface condition, its location on that surface's grid was randomized in a manner similar to the scheme presented in Table D1.

The experimental procedure was the same as in the calibration experiments, except that data were obtained manually instead of by computer DAS. Data were observed and recorded every 15 minutes. The HFS output varied considerably in short periods of time. It was therefore difficult to obtain a reading that would correspond to the average reading that a computer would obtain.

Analysis of the results revealed no bias as a function of sequence of experiments. Averaging all sensor treatments (Fig. D2) revealed little change in sensor calibration as a function of surface type. More change was apparent with the introduction of higher-thermal-resistance material (treatment H had only ⅔ as much heat flow through the HFS as treatment L). However, this may be due to the increased difficulty in reading the HFS output when the signal was affected more by convection currents and less by conduction through the thicker material. Plywood or gypsum covers eliminated the effect of convection and caused steady sensor readings.

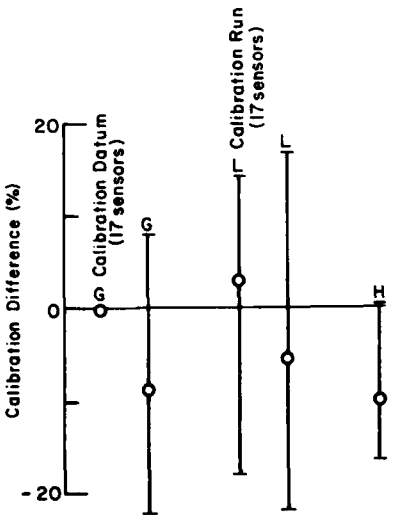

Figure D4. Difference in sensitivity of ITI sensors with tape covers for three wall conditions compared to an independent calibration. The calibration runs employed the DAS, whereas the sensitivity tests were recorded by hand; this is a probable source of bias between the two sets of data.

A summary of selected sensor and treatment conditions (Fig. D3) echoes this apparent tendency for high R-value (H) to have a higher *Cal.* Looking at just the taped ITI sensors that simulate the method used at Ft. Devens (Fig. D4), we see that the average apparent calibration for *G*, according to eq 2, should fall on the horizontal axis because such results have been normalized to the wallboard calibration obtained in the earlier calibration runs. However, it is displaced below where we should expect it. The L condition results are displaced an equivalent distance in the sensitivity tests, when compared with the calibration test. For these sensors, the H condition is slightly lower than the other two.

These somewhat contradictory results qualify only as a strong indication that experimental error is a stronger factor than change in surface material. The inconsistency between the two sets of experiments, calibration and sensitivity, is probably due to the difficulty in reading the fluctuating HFS output by eye.

The most practical result of the sensitivity tests is the prospect for calibrating sensors in small laboratory thermal testing machines, such as the C518 heat flow meters or the C177 guarded hot box (ASTM 1984). Figure D5 compares the results of ITI sensors, covered with tape and calibrated on wallboard in the large-scale calibrated hot box, with those calibrated in the same machine with a wallboard cover. The difference is minimal. Likewise the results obtained with Hycal sensors calibrated in a heat flow meter apparatus are only 5% above the calibration figures obtained in the calibrated hot box. Therefore, the smaller laboratory equipment may be adequate for calibration where the HFS will be sandwiched between a cover and construction surfaces of the same materials employed in the test apparatus.

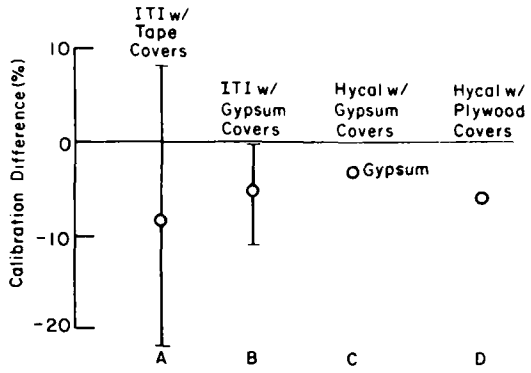

Figure D5. Difference in calibration between a value obtained to test sensitivity of the sensor to different thermal surroundings and a previously obtained reference calibration value. For A and B the reference calibrations were in the large calibrated hot box. For C and D the reference calibrations were in an ASTM C518 heat flow meter apparatus.

APPENDIX E: PLOTTED DATA FROM FT. DEVENS BUILDINGS

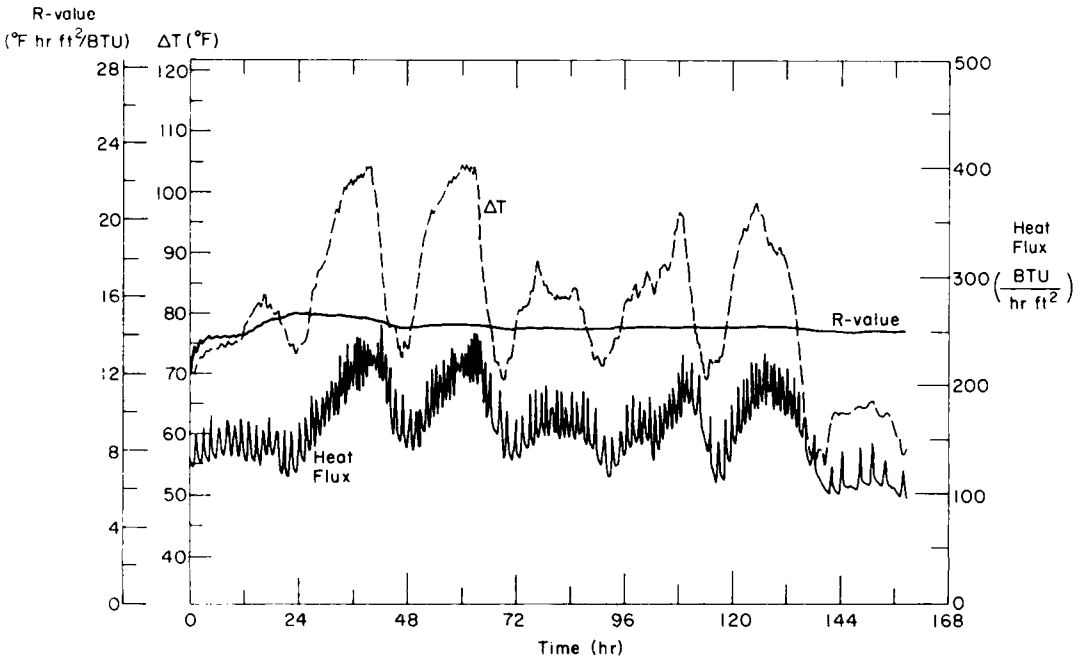

Figure E1. Temperature difference, heat flux and R_e for a frame wall of building 933. The ΔT data show a 24-hour variation attributable to daily change in outdoor temperature and a more frequent (about 40 min) cycle of the heating plant. The heat flux data lag slightly behind the ΔT data, but reflect the shape of the diurnal variation. The line depicting R_e quickly becomes stable for this light construction and this strong average ΔT.

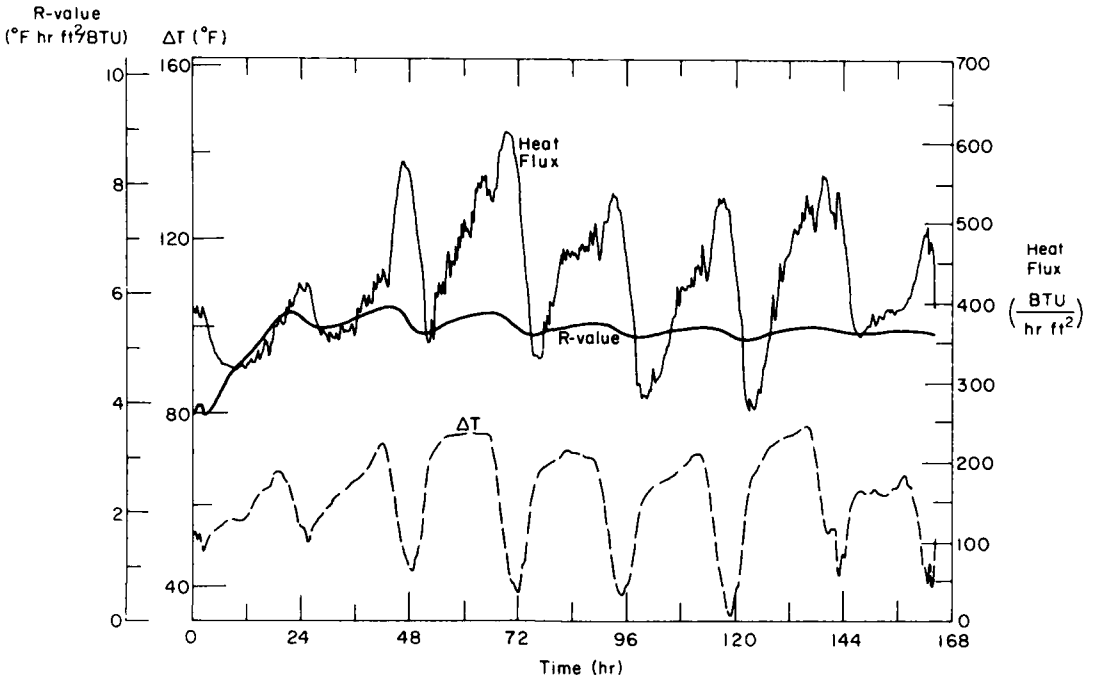

Figure E2. Temperature difference, heat flux and R_e for a concrete masonry wall of building 22. The massiveness of the construction causes heat flux to lag behind ΔT much more than for building 933 (Fig. E1). This fact and the lower average ΔT cause R_e to stabilize on a value more slowly.

A facsimile catalog card in Library of Congress MARC format is reproduced below.

Flanders, Stephen N.
Measuring thermal performance of building envelopes: Nine case studies / by Stephen N. Flanders. Hanover, N.H.: Cold Regions Research and Engineering Laboratory; Springfield, Va.: available from National Technical Information Service, 1985.
iv, 42 p., illus.; 28 cm. (CRREL Report 85-7.)
Prepared for Office of the Chief of Engineers by Corps of Engineers, U.S. Army Cold Regions Research and Engineering Laboratory under DA Project 4A762730 AT42.
Bibliography: p. 23.
1. Cost analysis. 2. Economic analysis. 3. Heat flow sensors. 4. Insulation. 5. Life cycle costs.

(cont'd on card 2)

(CARD 2)
Flanders, Stephen N.
Measuring thermal performance... 1985
6. Thermal insulation. 7. Thermal measurement. I. United States. Army. Corps of Engineers. II. Cold Regions Research and Engineering Laboratory, Hanover, N.H. III. Series: CRREL report 85-7.

END

FILMED

7-85

DTIC